Use of Oligodeoxyribonucleotides with Conformationally Constrained Abasic Sugar Targets To Probe the Mechanism of Base Flipping by *Hha*I DNA (Cytosine C5)-methyltransferase

Peiyuan Wang,[||,†] Adam S. Brank,[||,‡] Nilesh K. Banavali,[||,§] Marc C. Nicklaus,[†] Victor E. Marquez,*[,†] Judith K. Christman,*[,‡] and Alexander D. MacKerell, Jr.*[,§]

Contribution from the Laboratory of Medicinal Chemistry, Division of Basic Sciences, National Cancer Institute, NIH, Bethesda, Maryland 20892, Department of Biochemistry and Molecular Biology and UNMC/Eppley Cancer Center, 984525 University of Nebraska Medical Center, Omaha, Nebraska 68198-4525, and Department of Pharmaceutical Sciences, School of Pharmacy, University of Maryland, Baltimore, Maryland 21201

Received June 5, 2000

Abstract: X-ray crystallographic studies of *Hha*I DNA (cytosine-C5)-methyltransferase (M.*Hha*I) covalently linked to methylated 5-fluorocytosine in DNA provided the first direct evidence that the cytosine residue targeted for methylation was "flipped" out of the helix during the transfer reaction. Subsequent studies indicated that removal of the target cytosine base, i.e., introduction of an abasic site, enhanced binding of M.*Hha*I to DNA and that the conformation of the sugar−phosphate backbone at the abasic site in the resultant complexes was the same as that of the sugar attached to a "flipped" cytosine. In the present study, pseudorotationally constrained sugar analogues, based on bicyclo[3.1.0]hexane templates, were placed in DNA duplexes as abasic target sites in the M.*Hha*I recognition sequence. Biochemical studies demonstrate that binding affinity of M.*Hha*I for abasic sites increases when the abasic target sugar analogue is constrained to the south conformation and decreases when it is constrained to the north conformation. In native gel-shift assays, M.*Hha*I exhibits a "closed" conformation when bound to the abasic south or abasic furanose analogues, whereas an "open" conformation predominates with the abasic north analogue. A structural understanding of these results was obtained via molecular dynamics simulations of the DNA duplex alone and in ternary complex with M.*Hha*I and cofactor, along with quantum mechanical calculations on model compounds representative of the abasic and modified sugars. Binding affinities are shown to be related to the ability of the abasic sugar analogues to spontaneously flip out of the DNA duplex. Enhanced binding of the abasic south analogue is suggested to be due to its increased capacity for sampling the experimentally observed conformation of the DNA target site in the M.*Hha*I ternary complex. Decreased binding of the north analogue is due to decreased flexibility of the phosphodiester backbone associated with a north pseudorotation angle, thereby inhibiting spontaneous flipping of the sugar moiety out of the DNA duplex. Spontaneous flipping of the sugar moiety out of the DNA duplex is also suggested to facilitate formation of a "closed" complex between M.*Hha*I and DNA whereas partial or no flipping favors the "open" conformation. These results show that introduction of structural constraints into DNA that induce enhanced sampling of protein-bound conformations facilitate DNA−protein binding. Implications of the present results with respect to the mechanism of base flipping in the M.*Hha*I catalytic cycle are discussed.

Introduction

One of the hallmarks of DNA (cytosine C5)-methyltransferases from *Hha*I and *Hae*III is extrusion of a base from a B-DNA helix into the active site of the enzyme by a base flipping mechanism.[1,2] Many DNA glycosylases that remove abnormal bases from DNA have also been reported to use a base flipping mechanism to exert their action.[3−7] During the flipping process, the base is rotated completely out of the helix, breaking the corresponding Watson−Crick base pair and interrupting base stacking. Two mechanisms have been proposed for this process: (1) an active process in which the enzyme first pushes the base out of the helix and then pulls it into the active site of the enzyme and (2) a passive process in which a spontaneously formed extrahelical base is trapped by the protein during the normal breathing of the DNA.[8]

* To whom correspondence should be addressed: (e-mail) marquez@dc37a.nci.nih.gov; jchristm@unmc.edu; alex@outerbanks.umaryland.edu..

|| The first three authors contributed equally to the present work and should all be considered as first authors.

† National Cancer Institute.

‡ University of Nebraska Medical Center.

§ University of Maryland.

(1) Klimasauskas, S.; Kumar, S.; Roberts, R. J.; Cheng, X. *Cell* **1994**, *76*, 357−369.

(2) Reinisch, K. M.; Chen, L.; Verdine, G. L.; Lipscomb, W. N. *Cell* **1995**, *82*, 143−153.

(3) Lau, A. Y.; Scharer, O. D.; Samson, L.; Verdine, G. L.; Lipscomb, W. N. *Cell* **1998**, *95*, 249−258.

(4) Vassylyev, D. G.; Kashiwagi, T.; Mikani, Y.; Ariyoshi, M.; Iwai, S.; Ohtsuka, E.; Morikawa, K. *Cell* **1998**, *95*, 773−782.

(5) Savva, R.; McAuley-Hecht, K.; Brown, T.; Pearl, L. *Nature* **1995**, *373*, 487−493.

(6) Slupphaug, G.; Mol, C. D.; Kavli, B.; Arvai, A. S.; Krokan, H. E.; Tainer, J. A. *Nature* **1996**, *384*, 87−92.

(7) Barrett, T. E.; Savva, R.; Panayotou, G.; Barlow, T.; Brown, T.; Jiricny, J.; Pearl, L. H. *Cell* **1998**, *92*, 117−129.

10.1021/ja001989s CCC: $19.00
Published on Web 12/01/2000

From a comparison of NMR data and gel electrophoretic behavior, it has been proposed that at least three protein−DNA complexes are involved in the structural mechanism of action: (a) an initial complex formed between the enzyme and a normally stacked B-DNA helix, (b) an "open" complex of enzyme and DNA which is comprised of an "ensemble of flipped-out confomers", and (c) a more compact or "closed" complex in which the active site loop of the enzyme locks the flipped-out target cytosine into the active site pocket.[9] The first two complexes appear to be the major contributors in a dynamic equilibrium between the three states until cofactor binding shifts the equilibrium in favor of the final complex.[9] No experimentally derived structural information is available for the first two binary complexes although model structures have been constructed.[9]

Because the binding affinity of M.*Hha*I for its recognition sequence in DNA is inversely related to the stability of the target base pair, the first two complexes are proposed to be the major determinants of binding affinity between enzyme and substrate until cofactor binding shifts the equilibrium toward formation of the closed complex. The tightest binding of M.*Hha*I occurs when either the target base or the target nucleotide with both its 5′- and 3′-phosphates is missing (abasic site or gap).[10] Crystallographic analysis of ternary complexes containing M.*Hha*I, the cofactor *S*-adenosylhomocysteine (AdoHcy), and DNA containing an abasic target site revealed that the flexible abasic furanose sugar is in the flipped-out conformation.[11] The sugar adopts a ring pucker pseudorotation angle of 33°,[11] characteristic of a north conformation in the pseudorotational cycle.[12,13] In B-DNA, the sugar moieties favor pseudorotation angles of ∼160°, characteristic of the south conformation.[14] These observations suggested to us that studies of the effects of target abasic sugars with different conformational constraints on the interaction between M.*Hha*I and DNA would help to elucidate the nature of the DNA−protein interactions and their role in the mechanism of enzyme action.

Marquez and co-workers have designed and synthesized conformationally rigid nucleosides based on a bicyclo[3.1.0]-hexane template to study the importance of ring pucker for recognition and binding by various nucleoside and nucleotide processing enzymes.[15−31] In the present study, a logical extension of this approach was utilized to synthesize DNA fragments

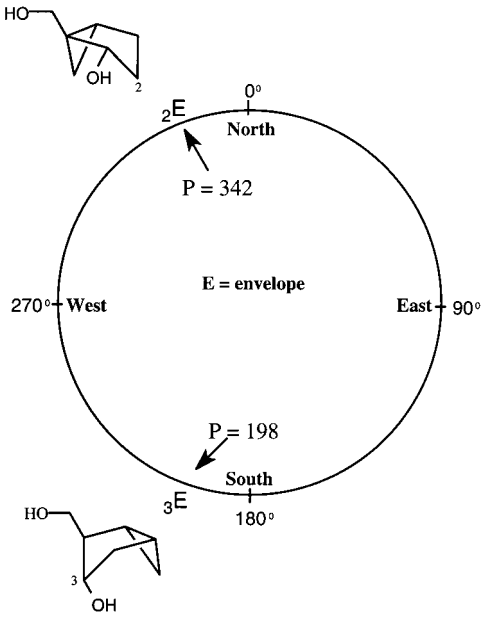

Figure 1. Conformationally constrained location of the bicyclo[3.1.0]-hexane templates in the sugar pseudorotation cycle.[13]

Scheme 1. (A) Sequence of the ds 13-Mer Oligonucleotide Used in the Biochemical Experiments (M = C5-Methylated Cytosine, X = Abasic Sugar). (B) Sequence of Double-Stranded 12-Mer Used for MD Simulations

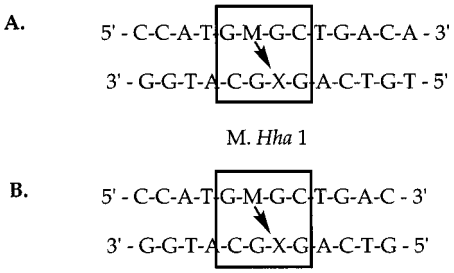

(oligodeoxyribonucleotides, ODNs; see Scheme 1) containing conformationally rigid abasic sugars (*X*) in place of the target C residue in the M.*Hha*I recognition sequence (5′-G*X*GC-3′). When the complementary strand contains a 5-methylcytosine (*M* in the sequence 5′-G*M*GC-3′) the residue *X*, indicated by an arrow in Scheme 1, becomes the only target for flipping. Incorporation of the sugars locked in one of the two antipodal hemispheres of the pseudorotational cycles (Figure 1) was accomplished by using the phosphoramidites **5** and **15** (Schemes 1 and 2 of the Supporting Information). Structures of the ODNs

(8) Roberts, R. J.; Cheng, X. *Annu. Rev. Biochem.* **1998**, *67*, 181−198.
(9) Klimasauskas, S.; Szyperski, T.; Serva, S.; Wuthrich, K. *EMBO J.* **1998**, *17*, 317−324.
(10) Klimasauskas, S.; Roberts, R. J. *Nucleic Acids Res.* **1995**, *23*, 1388−1395.
(11) O'Gara, M.; Horton, J. R.; Roberts, R. J.; Cheng, X. *Nat. Struct. Biol.* **1998**, *5*, 872−877.
(12) Altona, C.; Sundaralingam, M. *J. Am. Chem. Soc.* **1972**, *94*, 8205−8212.
(13) Saenger, W. *Principles of Nucleic Acid Structure*; Springer-Verlag: New York, 1984.
(14) Plavec, J.; Thibadeau, C.; Chattopadhyaya, J. *Pure Appl. Chem.* **1996**, *68*, 2137−2144.
(15) Rodriguez, J. B.; Marquez, V. E.; Nicklaus, M. C.; Barchi, J. J., Jr. *Tetrahedron Lett.* **1993**, *34*, 6233.
(16) Rodriguez, J. B.; Marquez, V. E.; Nicklaus, M. C.; H., M.; Barchi, J. J., Jr. *J. Med. Chem.* **1994**, *37*, 3389−3399.
(17) Ezzitouni, A.; Barchi, J. J., Jr.; Marquez, V. E. *J. Chem. Soc., Chem. Commun.* **1995**, 1345.
(18) Jeong, L. S.; Marquez, V. E.; Yuan, C.-S.; Borchardt, R. T. *Heterocycles* **1995**, *41*, 2651.
(19) Siddiqui, M. A.; Ford, H., Jr.; George, C.; Marquez, V. E. *Nucleosides Nucleotides* **1996**, *15*, 235.
(20) Jeong, L. S.; Marquez, V. E. *Tetrahedron Lett.* **1996**, *37*, 2353.
(21) Ezzitouni, A.; Marquez, V. E. *J. Chem. Soc., Perkin Trans. 1* **1997**, 1073.
(22) Ezzitouni, A.; Russ, P.; Marquez, V. E. *J. Org. Chem.* **1997**, *62*, 4870.
(23) Marquez, V. E.; Ezzitouni, A.; Siddiqui, M. A.; Russ, P.; Ikeda, H.; George, C. *Nucleosides Nucleotides* **1997**, *16*, 1431−1434.
(24) Marquez, V. E.; Ezzitouni, A.; Russ, P.; Siddiqui, M. A.; Ford, H., Jr.; Feldman, R. J.; Mitsuya, H.; George, C.; Barchi, J. J., Jr. *J. Am. Chem. Soc.* **1998**, *120*, 2780−2789.
(25) Marquez, V. E.; Ezzitouni, A.; Russ, P.; Siddiqui, M. A.; Ford, J., H.; Feldman, R. J.; Mitsuya, H.; George, C.; Barchi, J., J. J. *Nucleosides Nucleotides* **1998**, *17*, 1881−1884.
(26) Jeong, L. S.; Buenger, G.; McCormack, J. J.; Cooney, D. A.; Hao, Z.; Marquez, V. E. *J. Med. Chem.* **1998**, *41*, 2572−2578.
(27) Bekiroglu, S.; Thibadeau, C.; Kumar, A.; Matsuda, A.; Marquez, V. E.; Chattopadhyaya, J. *J. Org. Chem.* **1998**, *63*, 5447−5462.
(28) Moon, H. R.; Kim, H. O.; Chun, M. W.; Jeong, L. S.; Marquez, V. E. *J. Org. Chem.* **1999**, *64*, 4733−4741.
(29) Marquez, V. E.; Russ, P.; Alonso, R.; Siddiqui, M. A.; Shin, K. J.; George, C.; Nicklaus, M.; Dai, F.; Ford, J., H. *Nucleosides Nucleotides* **1999**, *18*, 521−530.
(30) Nandanan, E.; Jang, S.-Y.; Moro, S.; Kim, H.; Siddiqui, M. A.; Russ, P.; Marquez, V. E.; Busson, R.; Herdewjin, P.; Harden, T. K.; Boyer, J. L.; Jacobson, K. A. *J. Med. Chem.* **2000**, *43*, 829−842.
(31) Marquez, V. E.; Russ, P.; Alonso, R.; Siddiqui, M. A.; Hernandez, S.; George, C.; Nicklaus, M. C.; Dai, F.; Ford, J., H. *Helv. Chim. Acta* **1999**, *82*, 2119−2129.

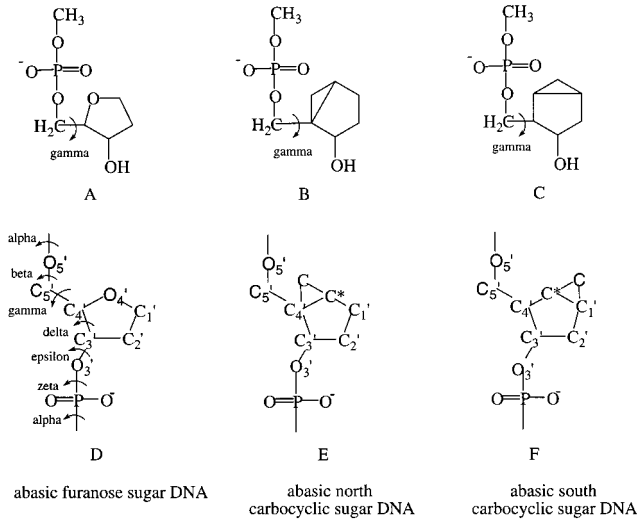

Figure 2. Model compounds used to study the γ-dihedral energy surface in the abasic sugar moieties (A−C) and representations of the abasic sugar moieties substituted in the DNA backbone (D−F). Compound A, abasic furanose moiety; compound B, abasic north carbocyclic moiety; compound C, abasic south carbocyclic moiety. The dihedral degrees of freedom indicated by curved arrows in D are named according to the standard convention for nucleic acids.[13]

containing sugar analogues in place of the target base *X* are represented in Figure 2E and F, with the abasic furanose ODN structure represented in Figure 2D. The stability of these ODN duplexes was determined and compared to the control ODN by melting temperature measurements. The interaction of the ODNs with M.*Hha*I was characterized by determining their capacity to inhibit methyl transfer from *S*-adenosylmethionine (AdoMet) to target C residues in normal substrates and by nondenaturing polyacrylamide gel-shift analysis of complexes formed between M.*Hha*I and the ODNs in the presence and absence of the cofactors, AdoHcy and AdoMet. Computational studies were used to understand the conformational behavior of the abasic ODNs in both aqueous solution and the protein-bound ternary complex. The impact of the conformational properties of the abasic sugar on interactions of M.*Hha*I with its substrates can be explained on the basis of experimental and theoretical results and is discussed within the general context of base flipping in the M.*Hha*I catalytic cycle.

Methods

1. Synthetic Methods. All chemical reagents were commercially available. Melting points were determined on a Mel-temp II apparatus and are uncorrected. Column chromatography was performed on silica gel 60, 230−400 mesh (E. Merck), analytical TLC was performed on Analtech Uniplates silica gel GF. Routine IR, and ^{1}H and ^{13}C NMR spectra were recorded using standard methods on a Bruker AC-250 instrument at 250 MHz. ^{31}P NMR spectra were recorded on a Bruker AMX500 using an inverse broad-band probe and were referenced to external trimethyl phosphate. Specific rotations were measured in a Perkin-Elmer model 241 polarimeter. Positive-ion fast-atom bombardment mass spectra (FABMS) were obtained on a VG 7070E mass spectrometer at an accelerating voltage of 6 kV and a resolution of 2000. Glycerol was used as the sample matrix, and ionization was effected by a beam of xenon atoms. Elemental analyses were performed by Atlantic Microlab, Inc., Norcross, GA.

***(1R,2R,3S,5R)*-2-[(Phenylmethoxy)methyl]bicyclo[3.1.0]hexan-3-ol (2).** A stirred solution of **1**[23] (2 g, 9.8 mmol) in dry CH_2Cl_2 (81 mL) was cooled at 0 °C and treated dropwise with Et_2Zn (1 M solution in hexane, 10.9 mL). After the addition, the reaction mixture was stirred for 15 min. Separately, CH_2I_2 (1.8 mL, 22.6 mmol) was dissolved in dry CH_2Cl_2 (10 mL) and half of this solution was added rapidly to the reaction mixture. After 5 min, additional Et_2Zn in hexane (10.9 mL) was added dropwise followed by the remaining half of the CH_2I_2 solution. The reaction mixture was stirred cold for ∼16 h and gradually allowed to reach room temperature. It was cooled again over ice, poured into 200 mL of aqueous saturated NH_4Cl, and extracted with EtOAc (3 × 250 mL). The combined organic extract was washed with aqueous saturated NH_4Cl, dried ($MgSO_4$), and filtered. The filtrate was concentrated to dryness, and the residue was purified by column chromatography on silica gel with hexanes and EtOAc (20:1) to give **2** (1.51 g, 70.6%) as a syrup: $[\alpha]^{25}_D$ 19.8° (*c* 0.57, MeOH); ^{1}H NMR ($CDCl_3$) δ 7.36 (m, 5 H, PhH), 4.54 (s, 2 H, PhC*H*$_2$O), 4.20 (d, J = 6.8 Hz, 1 H, H-3), 3.45 (dd, J = 9.0, 6.1 Hz, 1 H, $PhCH_2OCHH$), 3.27 (t, J = 8.8 Hz, 1 H, $PhCH_2OCHH$), 2.09−2.20 (m, 2 H, H-2 and H-4$_a$), 1.77 (br s, 1 H, OH), 1.65 (dd, J = 14.2, 1.5 Hz, 1 H, H-4$_b$), 1.27 (m, 1 H, H-1 or H-5), 1.12 (uneven quartet, 1 H, H-5 or H-1), 0.59 (m, 2 H, H-6$_{a,b}$); FAB MS *m*/*z* (relative intensity) 219 (MH^+, 41), 91 ($PhCH_2^+$, 100). Anal. Calcd for $C_{14}H_{18}O_2$·0.04H_2O: C, 76.78; H, 8.32. Found: C, 76.48; H, 8.34.

***(1R,2R,3S,5R)*-2-(Hydroxymethyl)bicyclo[3.1.0]hexan-3-ol (3).** To a stirred solution of Pd black (2 g) in MeOH (60 mL) was added a solution of **2** (1.06 g, 4.9 mmol) in MeOH (30 mL). Formic acid (96%, 6 mL) was added, and the reaction mixture was stirred at 50−55 °C for 1.5 h. The reaction mixture was filtered through Celite, and the filtrate was concentrated to dryness. The residue was purified by column chromatography on silica gel with 20 → 40% EtOAc in hexanes to give **3** (0.434 g, 70%) as a solid: mp 68−69 °C; $[\alpha]^{25}_D$ 42.5 ° (*c* 0.16, MeOH); ^{1}H NMR ($CDCl_3$) δ 4.24 (d, J = 6.8 Hz, 1 H, H-3), 3.65 (dd, J = 10.6, 5.9, Hz, 1 H, $PhCH_2OCHH$), 3.45 (dd, J = 10.5, 8.3 Hz, 1 H, $PhCH_2OHH$), 2.18 (m, 1 H, H-2), 2.05 (m, 1 H, H-4$_a$), 1.94 (br s, 2 H, OH), 1.67 (d, 14.2 Hz, 1 H, H-4$_b$), 1.39 and 1.22 (multiplets, 2 H, H-1, and H-5), 0.60 (m, 2 H, H-6$_{a,b}$); FAB MS of the diacetate derivative *m*/*z* (relative intensity) 213 (MH^+, 61), 153 (MH^+ − AcOH, 100). Anal. Calcd for $C_7H_{12}O_2$: C, 65.50; H, 9.44. Found: C, 65.53; H, 9.51.

***(1R,2R,3S,5R)*-2-[[Bis(4-methoxyphenyl)phenylmethoxy]methyl]-bicyclo[3.1.0]hexan-3-ol (4).** A solution of **3** (0.082 g, 0.6 mmol) in anhydrous CH_2Cl_2 (2.5 mL) containing DBU (0.25 mL, 1.64 mmol) was treated with 4,4′-dimethoxytrityl chloride (0.30 g, 0.8 mmol) at 0 °C. The reaction mixture was then stirred at room temperature for 14 h. It was then concentrated, and the residue was purified by column chromatography on silica gel with hexanes/EtOAc/Et_3N (gradient from 94:4:2 to 90:8:2) to give **4** (0.25 g, 91%) as a syrup: $[\alpha]^{25}_D$ 18.89° (*c* 0.19, EtOAc); ^{1}H NMR ($CDCl_3$) δ 6.82−7.47 (m, 13 H, ArH), 4.19 (d, J = 5.6 Hz, 1 H, H-3), 3.80 (s, 6 H, 2OCH_3), 3.13 (dd, J = 8.8, 6.1 Hz, 1 H, DMTOC*H*H), 2.93 (t, J = 8.3 Hz, 1 H, DMTOCH*H*), 2.13 and 2.06 (multiplets, 2 H, H-2 and H-4$_a$), 1.60 (dd, J = 13.9, 1.5 Hz, 1 H, H-4$_b$), 1.41, 1.27, and 1.14 (multiplets, 3 H, H-1, H-5, and H-6$_a$), 0.60 (m, 1 H, H-6$_b$); FAB MS *m*/*z* (relative intensity) 430.4 ($MH^{\bullet+}$, 6), 303 (trityl cation, 100). Anal. Calcd for $C_{28}H_{30}O_2$·0.6H_2O: C, 76.20; H, 7.13. Found: C, 76.08; H, 7.07.

***(1R,2R,3S,5R)*-3-[[2{[Bis(4-methoxyphenyl)phenylmethoxy]methyl]-bicyclo[3.1.0]hex-3-yloxy][bis(methylethyl)amino]phosphinooxy}-propanenitrile (5).** To a solution of **4** (0.082 g, 0.2 mmol) in anhydrous CH_2Cl_2 (5 mL) containing *N*,*N*-diisopropylethylamine (0.184 mL, 1.1 mmol) was added 2-cyanoethyl *N*,*N*-diisopropylchlorophosphoramidite (0.118 mL, 0.5 mmol) at 0 °C. The reaction mixture was stirred at 0 °C for 1 h and then at room temperature for an additional hour. After cooling again to 0 °C, the reaction was quenched with MeOH (1.5 mL) and concentrated to dryness under vacuum. The residue was purified by column chromatography on silica gel with hexanes/EtOAc/Et_3N (gradient from 95:3:2 to 93:5:2) to give **5** (0.092 g, 77%) as a syrup: FAB MS *m*/*z* (relative intensity) 303 (trityl cation, 100), 102 [(*i*-Pr)$_2NH_2^+$, 67); ^{31}P NMR ($CDCl_3$) δ 144.23 and 144.34.

***(1S,2S,3R,4S)*-4-(2,2-Dimethyl-1,1-diphenyl-1-silapropoxy)-3-[(phenylmethoxy)methyl]-2-(phenylselenamethyl)cyclopentan-1-ol (8).** A mixture of **6**[22] (0.788 g, 1.8 mmol) and PhSeCl (0.404 g, 2.1 mmol) in anhydrous DMSO (5 mL) was stirred under argon for 10 min at room temperature and then cooled to 0 °C. Silver trifluoroacetate (0.465 g, 2.1 mmol) was added, and the reaction mixture was stirred at room temperature for 12 h after which time TLC analysis (hexanes/benzene, 4:3) indicated no starting material present (R_f = 0.51). The reaction mixture containing crude **7** was treated with 5% NaOH in 95% EtOH

(9 mL) at 0 °C, stirred at room temperature for 30 min, poured into ice water (25 mL), and extracted with Et_2O (3 × 25 mL). The combined organic extract was washed with brine, dried ($MgSO_4$), and filtered. The filtrate was concentrated to dryness, and the residue was purified by column chromatography on silica gel with 5 → 8% EtOAc in hexanes to give **8** (0.882 g, 81.5%) as a syrup: $[\alpha]^{25}_D$ −12.66° (*c* 0.79, MeOH); ^{1}H NMR ($CDCl_3$) δ 7.10−7.62 (m, 20 H, Ph), 4.35 (m, 2 H, H-2, H-1), 4.21 (s, 2 H, PhC*H*$_2$O), 3.38 (dd, *J* = 9.3, 3.4 Hz, 1 H, H-4), 3.21 (t, *J* = 7.8 Hz, 1 H, $PhCH_2OCHH$), 3.09 (dd, *J* = 9.3, 3.2 Hz, 1 H, $PhCH_2OCHH$), 2.09−2.18 (m, 2 H, H-3, and H-5$_a$), 1.76 (m, 1 H, H-5$_b$), 1.02 (s, 9 H); FAB MS *m*/*z* (relative intensity) 617 (MH^+, 2), 599 ($MH^+ - H_2O$, 7.2), 91 ($PhCH_2^+$, 100). Anal. Calcd for $C_{35}H_{40}O_3SeSi$: C, 68.27; H, 6.55. Found: C, 68.00; H, 6.52.

***(1S,4S)*-4-(2,2-Dimethyl-1,1-diphenyl-1-silapropoxy)-3-[(phenylmethoxy)methyl]cyclopent-2-en-1-ol (9).** A solution of **8** (0.865 g, 1.4 mmol) and sodium metaperiodate (0.601 g, 2.8 mmol) in MeOH/water (9:1 v/v, 30 mL) was stirred at room temperature for 22 h. The reaction mixture was concentrated and coevaporated with EtOH to dryness. The residue was triturated with EtOAc (60 mL), and the white insolubles were removed by filtration. The filtrate was concentrated to dryness, and the residue was purified by column chromatography on silica gel with 10−15% EtOAc in hexanes to give **9** (0.470 g, 72.9%) as a syrup $[\alpha]^{25}_D$ −47.50° (*c* 0.12, EtOAc); ^{1}H NMR ($CDCl_3$) δ 7.29−7.67 (m, 15 H, PhH), 5.88 (s, 1 H, H-2), 5.04 (narrow multiplet, 1 H, H-1), 4.86 (narrow multiplet, 1 H, 4-H), 4.47 (s, 2 H, PhC*H*$_2$O), 4.10 (d, *J* = 13.7 Hz, 1 H, $PhCH_2OCHH$), 3.91 (d, *J* = 13.9 Hz, 1 H, $PhCH_2OCHH$), 2.11 (m, 1 H, H-5$_a$), 1.81 (m, 1 H, H-5$_b$), 1.50 (br s, 1 H, OH), 1.06 (s, 9 H, *tert*-butyl); FAB MS *m*/*z* (relative intensity) 459 (MH^+, 4), 441 ($MH^+ - H_2O$), 91 ($PhCH_2^+$, 100). Anal. Calcd for $C_{29}H_{34}O_3Si$: C, 75.94; H, 7.47. Found: C, 75.72; H, 7.54.

***(5S)*-[5-(2,2-Dimethyl-1,1-diphenyl-1-silapropoxy)cyclopent-1-enyl](phenylmethoxy)methane (10).** To a solution of **9** (1.426 g, 3.1 mmol) in anhydrous THF (15 mL) maintained under argon was added sulfur trioxide−pyridine complex (0.743 g, 4.67 mmol). The suspension was stirred at 0−3 °C for 3 h after which time analysis by TLC (hexanes/EtOAc, 3:1) indicated that the starting material had disappeared (R_f = 0.30). A solution of 1 M $LiAlH_4$ in THF (18.66 mL, 18.6 mmol) was added at 0 °C while stirring for 1 h. The reaction mixture was then allowed to reach 25 °C during the course of 3 h before quenching. Quenching of the reaction was performed at 0 °C by the successive addition of 0.7 mL of water, 0.7 mL of 15% aqueous sodium hydroxide, and 2 mL of water. Et_2O (131 mL) was added, and the precipitate formed was filtered and washed with additional organic solvent. The filtrate was concentrated to dryness, and the residue was purified by column chromatography on silica gel with 20% benzene in hexanes to give **10** (0.685 g, 50%) as a syrup: $[\alpha]^{25}_D$ −7.4° (*c* 0.50, EtOAc); ^{1}H NMR ($CDCl_3$) δ 7.29−7.73 (m, 15 H, PhH), 5.83 (s, 1H, H-2), 4.97 (uneven t, 1 H, H-5), 4.45 (s, 2 H, PhC*H*$_2$O), 4.08 (AB m, 2 H, $PhCH_2OCH_2$), 2.33 (m, 1 H, H-3$_a$), 2.1 (m, 1 H, H-3$_b$), 1.94 (m, 1 H, H-4$_a$), 1.77 (m, 1 H, H-4$_b$), 1.09 (s, 9 H, *tert*-butyl); FAB MS *m*/*z* (relative intensity) 441 ($MH^+ - H_2$, 5), 91 ($PhCH_2^+$, 100). Anal. Calcd for $C_{29}H_{34}O_2Si$: C, 78.68; H, 7.74. Found: C, 78.72; H, 7.80.

***(1S)*-2-[(Phenylmethoxy)methyl]cyclopent-2-en-1-ol (11).** Under an atmosphere of argon, a mixture of **10** (0.680 g, 1.5 mmol) in anhydrous acetonitrile (23 mL) was treated with triethylamine trihydrofluoride (98%, 1.48 mL) and heated at reflux for 10 h. After reaching room temperature, water (10 mL) was added and stirring was continued for 0.5 h. The reaction mixture was reduced to dryness, dissolved in a mixture of EtOH and benzene, and reconcentrated. The residue was purified by column chromatography on silica gel with 9% EtOAc in hexanes to give **11** (0.304 g, 100%) as a syrup: $[\alpha]^{25}_D$ 5.56° (*c* 0.14, MeOH); ^{1}H NMR ($CDCl_3$) δ 7.27−7.40 (m, 5 H, PhH), 5.86 (d, 1 H, *J* = 0.7 Hz, H-3), 4.87 (narrow multiplet, 1 H, H-1), 4.46 (s, 2 H, PhC*H*$_2$O), 4.21 (AB q, *J* = 10.9 Hz, 2 H, $PhCH_2OCH_2$), 2.52 (m, 1 H, H-4$_a$), 2.30 (m, 2 H, H-4$_b$, and H-5$_a$), 2.15 (br s, 1 H, OH), 1.80 (m, 1 H, H-5$_b$). Anal. Calcd for $C_{13}H_{16}O_2 \cdot 0.15H_2O$: C, 75.44; H, 7.94. Found: C, 75.29; H, 7.85.

***(1R, 2S, 5S)*-1-[(Phenylmethoxy)methyl]bicyclo[3.1.0]hexan-2-ol (12).** A stirred solution of **11** (0.200 g, 1.0 mmol) in dry CH_2Cl_2 (8 mL) was cooled at 0 °C and treated dropwise with Et_2Zn (1 M/hexane, 1.12 mL). After the addition, the reaction mixture was stirred for 15 min. Separately, CH_2I_2 (0.186 mL, 2.31 mmol) was dissolved in dry CH_2Cl_2 (1.7 mL), and half of this solution was added rapidly to the reaction mixture. After 5 min, an additional amount of Et_2Zn (1 M/hexane, 1.12 mL) was added dropwise followed by the remaining half of the CH_2I_2 solution. The reaction mixture was stirred cold for ∼16 h and gradually allowed to reach room temperature. It was cooled again over ice and poured into 20 mL of aqueous saturated NH_4Cl and extracted with EtOAc (3 × 25 mL). The combined organic extract was washed with aqueous saturated NH_4Cl, dried ($MgSO_4$), and filtered. The filtrate was concentrated to dryness, and the residue was purified by column chromatography on silica gel with 10% EtOAc in hexanes to give **12** (0.189 g, 88.3%) as a syrup: $[\alpha]^{25}_D$ 16.45 ° (*c* 0.93, MeOH); ^{1}H NMR ($CDCl_3$) δ 7.28−7.36 (m, 5 H, PhH), 4.52−4.58 (m, 3 H, H-2, and PhC*H*$_2$O), 3.76 (d, *J* = 9.8 Hz, 1 H, $PhCH_2OCHH$), 3.42 (d, *J* = 9.8 Hz, 1 H, $PhCH_2OCHH$), 2.00−1.85 (m, 2 H, H-3$_a$, and OH), 1.71−1.81 (m, 2 H, H-3$_b$, and H-4$_a$), 1.21 (m, 2 H, H-5, and H-4$_b$), 0.94 (t, *J* = 4.4 Hz, 1 H, H-6$_b$), 0.45 (dd, *J* = 7.8, 5.4 Hz, 1 H, H-6$_b$); FAB MS *m*/*z* (relative intensity) 219 (MH^+, 21), 210 ($MH^+ - H_2O$, 17), 93 [MH^+ − ($PhCH_2OH + H_2O$), 100]. Anal. Calcd for $C_{14}H_{18}O_2$: C, 77.03; H, 8.31. Found: C, 77.15; H, 8.32.

***(1R, 2S, 5S)*-1-(Hydroxymethyl)bicyclo[3.1.0]hexan-2-ol (13).** To a stirred suspension of Pd black (0.358 g) in MeOH (26 mL) was added a solution of **12** (0.164 g, 0.8 mmol) in MeOH (14 mL). Formic acid (96%, 0.9 mL) was added, and the reaction mixture was stirred at 50 °C for 1 h. After cooling to room temperature, the reaction mixture was filtered through Celite and the filtrate was concentrated to dryness. The residue was purified by column chromatography on silica gel with 30−50% EtOAc in hexanes to give **13** (0.077 g, 80%) as a syrup: $[\alpha]^{25}_D$ 2.5 ° (*c* 0.90, MeOH); ^{1}H NMR ($CDCl_3$) δ 4.59 (t, *J* = 8.2 Hz, 1 H, H-2), 3.96 (d, *J* = 10.7 Hz, 1 H, C*HH*OH), 3.56 (d, *J* = 11.2 Hz, 1 H, CH*H*OH), 1.72−2.02 (m, 3 H, H-4$_a$, H-3$_{a,b}$), 1.25 (m, 2 H, H-5, and H-4$_b$), 0.91 (t, *J* = 4.6 Hz, 1 H, H-6$_a$), 0.51 (dd, *J* = 87.8, 5.6 Hz, 1 H, H-6$_b$). Anal. Calcd for $C_7H_{12}O_2$: C, 65.60; H, 9.44. Found: C, 65.77; H, 9.48.

***(1R,2S,5S)*-1-{[Bis(4-methoxyphenyl)phenylmethoxy]methyl}-bicyclo[3.1.0]hexan-2-ol (14).** A solution of **13** (0.080 g, 0.6 mmol) in anhydrous CH_2Cl_2 (2.5 mL) containing DBU (0.23 mL, 1.6 mmol) was treated with 4,4′-dimethoxytrityl chloride (0.267 g, 0.8 mmol) at 0 °C. The reaction mixture was stirred for 6 h at room temperature and then concentrated under reduced pressure. The residue was purified by column chromatography on silica gel with hexanes/EtOAc/Et_3N (from 96:2:2 to 93:5:2) to give **14** (0.156 g, 58%) as a syrup: $[\alpha]^{25}_D$ 5.60 ° (*c* 0.25, EtOAc); ^{1}H NMR ($CDCl_3$) δ 6.82−7.47 (m, 13 H, PhH), 4.49 (t, *J* = 8.1 Hz, 1 H, H-2), 3.80 (s, 6 H, 2 OCH_3), 3.38 (d, *J* = 9.3 Hz, 1 H, DMTOC*H*HO), 3.07 (d, *J* = 9.3 Hz, 1 H, DMTOCH*H*O), 2.5 (br s, 1 H, OH), 1.93 (m, 1 H, H-4$_a$), 1.71 (m, 2 H, H-4$_b$, and H-3$_{a,b}$), 1.11−1.30 (m, 2 H, H-4$_b$, and H-5), 0.95 (t, *J* = 4.6 Hz, 1 H, H-6$_a$), 0.41 (dd, *J* = 7.8, 5.1 Hz, 1H, H-6$_b$); FAB MS *m*/*z* (relative intensity) 430 ($M^{\bullet+}$, 7), 303 (trityl cation, 100). Anal. Calcd for $C_{28}H_{30}O_4$: C, 78.11; H, 7.02. Found: C, 77.84; H, 7.18.

***(1R,2S,5S)*-3-{[1-[[Bis(4-methoxyphenyl)phenylmethoxy]methyl]-bicyclo[3.1.0]hex-2-yloxy][bis(methylethyl)amino]phosphinooxy}-propanenitrile (15).** To a solution of **14** (0.156 g, 0.4 mmol) in anhydrous CH_2Cl_2 (10 mL) containing *N*,*N*-diisopropylethylamine (0.38 mL, 2 mmol) was added 2-cyanoethyl *N*,*N*-diisopropylchlorophosphoramidite (0.242 mL, 1.0 mmol) at 0 °C. The reaction mixture was stirred at 0 °C for 1 h and then at room temperature for an additional hour. After the reaction was quenched with MeOH (1.5 mL) at 0 °C, it was concentrated to dryness under vacuum. The residue was purified by column chromatography on silica gel with hexanes/EtOAc/Et_3N (from 96:2:2 to 93:5:2) to give **15** (0.096 g, 42%) as a syrup: FAB MS *m*/*z* (relative intensity) 303 (trityl cation, 100), 102 [(*i*-Pr)$_2NH_2^+$, 15); ^{31}P NMR ($CDCl_3$) δ 144.75 and 145.59.

5′-TGT CAG XGC ATG G-3′ (ODN-south, X = South Bicyclo-[3.1.0]hexane Template, Scheme 1A). This oligo (15 OD units, 458 μg) was synthesized by Oligos Etc. Inc., Wilsonville, OR. The purity of the material was estimated to be >90.0% by capillary electrophoresis.

5′-TGT CAG XGC ATG G-3′ (ODN-north, X = North Bicyclo-[3.1.0]hexane template, Scheme 1A). This oligo (2.8 OD units, 85.5 μg) was synthesized by Oligos Etc. Inc. The purity of the material was estimated to be >90.0% by capillary electrophoresis.

2. Biochemical Methods. Binding Assays. For native gel-shift assays and determination of dissociation of M.*Hha*I−ODN complexes, reaction mixtures contained 30 nM ^{32}P-end-labeled duplex ODN, 30 nM M.*Hha*I, 75 ng of poly(dAdT:dAdT) to inhibit nonspecific binding, and 100 μM cofactor (as noted) in binding buffer (50 mM Tris (pH 7.5), 10 mM EDTA, 5 mM 2-mercaptoethanol, and 13% (v/v) glycerol). Complexes formed during a 30-min incubation at 22 °C were separated from free ODNs by electrophoresis at 150 V for 2.5−3 h on 10% polyacrylamide gels that had been pre-electrophoresed at 100 V for 1 h in TBE. To test complex stability, 100-fold molar excess of the same unlabeled ODN used in the initial binding reaction was added, and incubation continued for 1 min−5 days to determine the time required to exchange 50% of radiolabel in the complex ($T_{1/2}$). Gels were held at a constant temperature of 14 °C throughout electrophoresis. Dried gels were exposed to Phosphor Imager (Molecular Dynamics) screens, and the resulting images were used to quantitate radiolabeled ODNs in free and complexed form.

Inhibition Assays. Reaction mixtures (50 μL in 50 mM Tris (pH 7.5), 10 mM EDTA, and 5 mM 2-mercaptoethanol) contained 8.6 nM M.*Hha*I, 2.43 μM [^{3}H]-AdoMet (specific activity 15 Ci/mmol), 640 nM ds-ODN substrate, and increasing concentrations (0, 10, 25, 65, or 165 nM) of ds-ODNs containing furan, north- or south-bicyclo[3.1.0]-hexane pseudosugars at the target site. The substrate DNA, which contains a single M.*Hha*I recognition site, was formed from fully methylated ODN A (AMp) and unmethylated A′ by heating equimolar amounts of the two strands to 90 °C for 10 min and then slowly cooling to 50 °C for 60 min[32] (AMp, 5′-ATT**G*M*GC**ATTCMGGATCMGM-GATC-3′, and A′, 3′-TAA**CGCG**TAAGGCCTAGGCGCTAG-5′- M.*Hha*I; recognition site in boldface type, target underlined, *M* = 5-methylcytosine). The double-stranded (ds) ODNs with modified sugars were formed from ODN-south, ODN-north, or ODN-furan (5′TGTCA**G*X*GC**ATGG3′, M.*Hha*I site in boldface type, *X* indicates substituted target site) and its complement, 5′CCAT**G*M*GC**TGACA3′. Reactions were incubated at 37 °C for 5 min and terminated by the addition of NaOH to a concentration of 0.4 M. DNA was processed for quantitation of [^{3}H]-methyl incorporation as previously described.[32] Highly purified M.*Hha*I, used for all experiments reported here, was the generous gift of Dr. Xiaodong Cheng.[33]

Melting Temperature Determinations. ODN-north, ODN-south, ODN-furan, or ODN-C (cytosine in target site; see below) and the complementary ODN containing 5-mC at position 6 were taken up in 0.3 × SSC. The final concentration of each ODN was 1.5 ± 0.05 μM. The solutions were heated at 37 °C for 60 min and slowly cooled. Initial OD measurements indicated that these conditions allowed full annealing of the duplex. A Perkin-Elmer UV−visible spectrophotometer Lambda 10 was used to monitor changes in absorbance with each 0.1 °C change in temperature from 25 to 80 °C. Data from four cycles of melting and annealing were obtained for each of the four duplexes using PE Temp Lab software. T_m determinations were made from each cycle by graphic analysis of plots and confirmed by analysis of first-derivative data.

3. Computational Methods. Ab initio calculations were carried out using the Gaussian 94[34] or Gaussian 98[35] programs with the HF/6-31+G* basis set on model compounds A−C shown in Figure 2A−C. The definitions of the various dihedrals in the DNA backbone of the abasic systems are illustrated in Figure 2D. Model compounds A−C were chosen to obtain the γ dihedral energy surface in the three abasic sugar moieties included in this study. This surface was obtained by constraining the C3′−C4′−C5′−O5′ dihedral in 30° increments from 0 to 360°. In all cases, the following additional constraints were included: C−O−P−O5′ = 262°, O−P−O5′−C5′ = 298°, P−O5′−C5′−C4′ = 168°, and C4′−C3′−O3′−H = 187° while the remainder of the molecule was allowed to relax. These constraints correspond to modal values of the ζ, α, β, and ϵ crystallographic dihedral distributions in B-DNA[36] and are introduced to prevent variations in the other dihedral degrees of freedom from interfering with the γ energy surface, as previously performed.[37] For the abasic furanose, additional constraints were necessary to sample specific regions of the sugar psuedorotation surface: the C3′−C4′−O4′−C1′ dihedral was constrained to 0° to sample the C2′ endo conformation favored in B-DNA and the C4′−O4′−C1′−C2′ was constrained to 0° to sample the C3′ endo conformation favored in A-DNA.[37,38]

Molecular mechanics force field calculations were carried out using the CHARMM program,[39,40] and the analysis of DNA parameters was done using the FREEHELIX program[41] modified to read CHARMM-generated MD trajectories. The CHARMM27 parameters for DNA[36,42] and the CHARMM22 parameters for proteins[43] were used for all calculations along with the CHARMM-modified TIP3P water model[44,45] and the sodium parameters from Beglov and Roux.[46] New parameters had to be developed for the north and south carbocyclic sugar moieties. This was performed based on ab initio data on various model compounds representative of carbocyclic and abasic furanose sugar moieties in the context of their substitution into DNA.[47] The new parameters are included with the Supporting Information. Unique parameters for AdoHcy were generated by direct transfer of related parameters from the nucleic acid and protein sets.

MD simulations were carried out on two types of systems: (1) systems containing DNA alone in aqueous solution and (2) the partially solvated protein−DNA−cofactor ternary complex. The DNA and ternary complex MD simulations were each performed on four systems consisting of the DNA dodecamer sequence 5′-CCATGCGCTGAC-3′ (Scheme 1B, note the omission of the 3′-terminal position base pair in these calculations), hemimethylated at the position 6 cytosine of strand 1 (M in Scheme 1). The four systems consisted of (1) an unmodified cytosine base, (2) an abasic furanose sugar, (3) an abasic north

(32) Christman, J. K.; Sheikhnejad, G.; Marasco, C. J.; Sufrin, J. R. *Proc. Natl. Acad. Sci. U.S.A.* **1995**, *92*, 7347−7351.

(33) Kumar, S.; Cheng, X.; Pflugrath, J. W.; Roberts, R. J. *Biochemistry* **1992**, *31*, 8648−8653.

(34) Frisch, M. J.; Trucks, G. W.; Schlegel, H. B.; Gill, P. M. W.; Johnson, B. G.; Robb, M. A.; Cheeseman, J. R.; Raghavachari, K.; Al-Laham, M. A.; Zakrzewski, V. G.; Ortiz, J. V.; Foresman, J. B.; Cioslowski, J.; Stefanov, B. B.; Nanayakkara, A.; Challacombe, M.; Peng, C. Y.; Ayala, P. Y.; Chen, W.; Wong, M. W.; Andres, J. L.; Replogle, E. S.; Gomperts, R.; Martin, R. L.; Fox, D. J.; Binkley, J. S.; Defrees, D. J.; Baker, J.; Stewart, J. J. P.; Head-Gordon, M.; Gonzalez, C.; Pople, J. A. *Gaussian 94*, C.3 ed.; Gaussian, Inc.: Pittsburgh, PA, 1996.

(35) Frisch, M. J.; Trucks, G. W.; Schlegel, H. B.; Scuseria, G. E.; Robb, M. A.; Cheeseman, J. R.; Zakrzewski, V. G.; Montgomery, J. A., Jr.; Stratmann, R. E.; Burant, J. C.; Dapprich, S.; Millam, J. M.; Daniels, A. D.; Kudin, K. N.; Strain, M. C.; Farkas, O.; Tomasi, J.; Barone, V.; Cossi, M.; Cammi, R.; Mennucci, B.; Pomelli, C.; Adamo, C.; Clifford, S.; Ochterski, J.; Petersson, G. A.; Ayala, P. Y.; Cui, Q.; Morokuma, K.; Malick, D. K.; Rabuck, A. D.; Raghavachari, K.; Foresman, J. B.; Cioslowski, J.; Ortiz, J. V.; Stefanov, B. B.; Liu, G.; Liashenko, A.; Piskorz, P.; Komaromi, I.; Gomperts, R.; Martin, R. L.; Fox, D. J.; Keith, T.; Al-Laham, M. A.; Peng, C. Y.; Nanayakkara, A.; Gonzalez, C.; Challacombe, M.; Gill, P. M. W.; Johnson, B.; Chen, W.; Wong, M. W.; Andres, J. L.; Gonzalez, C.; Head-Gordon, M.; Replogle, E. S.; Pople, J. A. *Gaussian 98*, Revision A.6 ed.: Pittsburgh, PA, 1998.

(36) Foloppe, N.; MacKerell, A. D., Jr. *J. Comput. Chem.* **2000**, *21*, 86−104.

(37) Foloppe, N.; MacKerell, A. D., Jr. *J. Phys. Chem. B* **1999**, *103*, 10955−10964.

(38) Foloppe, N.; MacKerell, A. D., Jr. *J. Phys. Chem. B* **1998**, *102*, 6669−6678.

(39) Brooks, B. R., Bruccoleri, R. E., Olafson, B. D., States, D. J., Swaminathan, S., Karplus, M. J. *J. Comput. Chem.* **1983**, *4*, 187−217.

(40) MacKerell, A. D., Jr.; Brooks, B.; Brooks, C. L., III.; Nilsson, L.; Roux, B.; Won, Y.; Karplus, M. *CHARMM: The Energy Function and Its Parameterization with an Overview of the Program*; Schleyer, P. v. R.; Allinger, N. L.; Clark, T.; Gasteiger, J.; Kollman, P. A.; Schaefer, H. F., III; Schreiner, P. R., Eds.; John Wiley & Sons: Chichester, 1998; Vol. 1, pp 271−277.

(41) Dickerson, R. E. *Nucleic Acids Res.* **1998**, *26*, 1906−1926.

(42) MacKerell, A. D., Jr.; Banavali, N. *J. Comput. Chem.* **2000**, *21*, 105−120.

(43) MacKerell, A. D., Jr.; Bashford, D.; Bellott, M.; Dunbrack, R. L., Jr.; Evanseck, J.; Field, M. J.; Fischer, S.; Gao, J.; Guo, H.; Ha, S.; Joseph, D.; Kuchnir, L.; Kuczera, K.; Lau, F. T. K.; Mattos, C.; Michnick, S.; Ngo, T.; Nguyen, D. T.; Prodhom, B.; Reiher, I., W. E.; Roux, B.; Schlenkrich, M.; Smith, J.; Stote, R.; Straub, J.; Watanabe, M.; Wiorkiewicz-Kuczera, J.; Yin, D.; Karplus, M. *J. Phys. Chem. B* **1998**, *102*, 3586−3616.

(44) Jorgensen, W. L.; Chandrasekhar, J.; Madura, J. D.; Impey, R. W.; Klein, M. L. *J. Chem. Phys.* **1983**, *79*, 926−935.

(45) Reiher, W. E., III. *Theoretical Studies of Hydrogen Bonding*; Harvard University: Cambridge, MA, 1985.

(46) Beglov, D.; Roux, B. *J. Chem. Phys.* **1994**, *100*, 9050−9063.

(47) Banavali, N. K.; MacKerell, A. D., Jr., manuscript in preparation.

carbocyclic sugar analogue, and (4) an abasic south carbocyclic sugar analogue, all at position 6 of strand 2 (*X* in Scheme 1B) of the DNA. Systems 2, 3, and 4 correspond to Figure 2D, E, and F, respectively. The four DNA MD simulation systems will be referred to henceforth as ODN-C, ODN-furan, ODN-north, and ODN-south, respectively. The corresponding four protein−DNA−cofactor systems will be referred to as the ternary-C, ternary-furan, ternary-north, and ternary-south systems, respectively.

The abasic furanose and north carbocyclic and south carbocyclic sugars were generated from the canonical B-form of DNA[48] or from the DNA in the experimental ternary structure[11] by deletion of the cytosine base at position 6 of strand 2 and substitution with a hydrogen atom. For the conformationally constrained north and south carbocyclic sugars, the O4′ atom of the furan ring of the sugar was substituted with a carbon atom, and a cyclopropane ring was generated at the appropriate position as illustrated in Figure 2E and F.

Simulations of the DNA systems were initiated from canonical B-form DNA overlaid with a preequilibrated solvent box consisting of water and sodium ions, which extended at least 8.0 Å beyond the DNA solute. All solvent molecules having a non-hydrogen atom within 1.8 Å of the DNA were deleted. The number of sodium ions was adjusted to ensure electrostatic neutrality of the system by adding sodium ions at random positions in the box or deleting the sodium ions furthest from the DNA, as required. Periodic boundary conditions were used in all subsequent calculations with the images generated using the CRYSTAL module.[49] The system was minimized for 500 Adopted Basis Newton−Raphson (ABNR) steps with mass-weighted harmonic constraints of 2.0 kcal mol^{-1} Å^{-1} on the non-hydrogen DNA atoms. The minimized system was then subjected to a 20-ps constant volume, isothermal (NVT) ensemble MD simulation keeping the same harmonic constraints in order to equilibrate the solvent around the DNA. The resulting system was minimized for 500 ABNR steps without any constraints, and the final structure was used to initiate the production trajectories. Production MD simulations were performed for 2 ns in the isobaric, isothermal (NPT) ensemble[50] at 300 K with the Leapfrog integrator. All calculations were performed using SHAKE[51] to constrain covalent bonds containing hydrogen, using an integration time step of 0.002 ps, and treating long-range electrostatic interactions using the particle mesh Ewald (PME) approach.[52] PME calculations were performed using real space and Lennard-Jones (LJ) interaction cutoffs of 10 Å, with nonbond interaction lists maintained and heuristically updated out to 12 Å. The fast Fourier transform grid densities were set to ∼1 Å^{-1} using a fourth-order smoothing spline. The screening parameter (κ) was set to 0.35.

The experimental ternary abasic furanose M.*Hha*I−DNA−AdoHcy complex structure[11] was used as the starting point for the three abasic ternary complex simulations. The ternary-C simulation was initiated from the experimental ternary structure that has the cytosine base in the flipped orientation.[1] For all the ternary simulations, the starting structures were overlaid with a preequilibrated sodium−water sphere of radius 25 Å which was centered with respect to the two terminal C1′ atoms on strand 1 of the DNA. All solvent molecules having a non-hydrogen atom within 1.8 Å of DNA and 2.5 Å of protein non-hydrogen atoms were deleted. The number of sodiums was adjusted to yield a neutral system as mentioned above. Constraints applied throughout the subsequent calculations were as follows. Protein residues with one or more atoms outside the solvent sphere were fixed, and protein residues with one or more atoms in the concentric region of the solvent sphere extending from 21 to 25 Å radius were harmonically constrained using a 2.0 kcal mol^{-1} Å^{-1} mass-weighted force constant. A quartic spherical solvent boundary potential used to minimize artificial boundary conditions at the surface of the water sphere was applied to the water oxygen atoms using the miscellaneous mean field potential (MMFP) module[46] with an offset distance of 23.5 Å, a well depth of the potential of −0.25 kcal/mol, and the p1 parameter of the potential set to 2.25. The system was first minimized for 500 steepest descent (SD) steps with mass-weighted harmonic constraints of 2.0 kcal mol^{-1} Å^{-1} on the remaining unconstrained non-hydrogen DNA, protein, and AdoHcy atoms. The minimized system was then subjected to a 20-ps NVT MD simulation keeping the above-mentioned harmonic constraints in order to equilibrate the solvent around the complex. The resulting system was minimized for 500 SD steps without the additional constraints, and the final structure was used to initiate the production trajectories. Production MD simulations were performed for 2 ns in the NVT ensemble at 300 K with the Leapfrog integrator using the Nose−Hoover method for temperature scaling with the magnitude of coupling, q_{ref}, set to 100.0.[53,54] All calculations were performed using SHAKE[51] to constrain covalent bonds containing hydrogen, an integration time step of 0.002 ps, and treating long-range electrostatic interactions using atom truncation. Atom truncation was performed by using the force shift and force switch methods to truncate the electrostatic and LJ terms, respectively.[55] Nonbond interactions were heuristically updated, truncated at 12 Å with the switching function initiated at 10 Å, and the nonbond interaction lists maintained to 14 Å.

Analysis of the MD simulations was carried out on the last 1500 ps of the simulations, allowing 500 ps of equilibration time, unless otherwise stated. Averages and standard errors were calculated by dividing the data into five blocks of 300 ps each and carrying out statistical analysis on the block average values. The division of the data into individual 300-ps blocks is done with the assumption that each block is an independent sample of the MD trajectory and allows for calculation of statistical parameters that are not just representative of the fluctuations in the trajectory.[56]

C1′−C1′ and C4′−C4′ interstrand distances have previously been used to monitor the flipping-out transition in order to distinguish between sugar movements and backbone phosphate movements.[57] These two distances were observed to be highly correlated in the flipping out transition in that study. Since the O4′ atom connects the C1′ and C4′ atoms in the deoxyribose sugar, we chose the sugar O4′−O4′ interstrand distance between strand 1, residue 7 and strand 2, residue 6 as the single parameter to measure the extent of flipping. In the north and south sugars, the carbon atom used instead of the O4′ atom for the calculation of this distance corresponds to the C* atom shown in Figure 2. This distance will henceforth be referred to as the sugar O4′−O4′ distance. Residue 6 of strand 2 of the DNA is referred to as the flipped position with its sugar moiety being referred to as the flipped sugar. The residues adjacent to the flipped position on the 5′ side (strand 2, residue 5) and the 3′ side (strand 2, residue 7) are referred to as the 5′ position and the 3′ position, respectively.

Results

1. Synthetic Studies. (*1S,2R*)-2-[(Benzyloxy)methyl]cyclopent-3-enol (**1**) was selected as the chiral starting material for the synthesis of the conformationally locked south- and north-type phosphoramidites **5** and **15** (See text and Schemes 1 and 2 of the Supporting Information). Phosphoramidites **5** and **15** were used in a conventional DNA synthesizer to synthesize the two 13-mers containing the south (ODN-south) and north (ODN-north) abasic sites. The sequence of the target oligos synthesized corresponds to 5′-TGT CAG XGC ATG G-3′, where X is either the south or the north bicyclo[3.1.0]hexane template, respectively (Scheme 1A, strand 2). The coupling yields for the modified abasic pseudosugars were rather low; however, sufficient material was obtained to perform the necessary biological

(48) Arnott, S.; Hukins, D. W. L. *J. Mol. Biol.* **1973**, *81*, 93−105.
(49) Field, M. J.; Karplus, M. *CRYSTAL: Program for Crystal Calculations in CHARMM*; Harvard University: Cambridge, MA, 1992.
(50) Feller, S. E.; Zhang, Y.; Pastor, R. W.; Brooks, R. W. *J. Chem. Phys.* **1995**, *103*, 4613−4621.
(51) Ryckaert, J. P.; Ciccotti, G.; Berendsen, H. J. C. *J. Comput. Phys.* **1977**, *23*, 327−341.
(52) Darden, T. A.; York, D.; Pedersen, L. G. *J. Chem. Phys.* **1993**, *98*, 10089−10092.
(53) Nosé, S. *J. Chem. Phys.* **1984**, *81*, 511−519.
(54) Hoover, W. G. *Phy. Rev.* **1985**, *A31*, 1695.
(55) Steinbach, P. J.; Brooks, B. R. *J. Comput. Chem.* **1994**, *15*, 667−683.
(56) Loncharich, R. J.; Brooks, B. R.; Pastor, R. W. *Biopolymers* **1992**, *32*, 523.
(57) Barsky, D.; Foloppe, N.; Ahmadia, S.; Wilson, D. M., III; MacKerell, A. D., Jr. *Nucleic Acids Res.* **2000**, *28*, 2613−2626.

Table 1. Melting Temperatures and IC_{50} Values for the Inhibition of Methyltransferase Activity of M.*Hha*I by Oligodeoxynucleotides Containing a Cytosine (control) or Abasic Target

	melting temp[a] (°C)	IC_{50} value (nM)
1. control	56.1 (0.0)	nd[b]
2. furan	37.1 (0.2)	48
3. north	39.6 (0.3)	~180
4. south	38.2 (0.5)	14

[a] Standard deviations in parentheses. [b] nd, not determined as this ODN is a substrate.

experiments. Both double-stranded ODNs gave similar melting curves with T_m values comparable to a standard abasic double-stranded ODN containing tetrahydrofuran at the abasic site (Table 1 and Methods).

2. Biochemical Studies. Two approaches were used to determine the effect of conformational constraint of an abasic target site on the function of M.*Hha*I. The first was to compare the inhibitory capacity of abasic ds-ODNs-north, -south, and -furan. The second was to directly compare the extent to which M.*Hha*I could bind to each of the ds-ODNs in the presence and absence of cofactor and to determine whether the M.*Hha*I in binary or ternary complexes took on an "open" or "closed" conformation. Inhibition curves for M.*Hha*I methyltransferase activity (Figure 1 of Supporting Information) showed that ODN-south has the highest inhibitory activity with an IC_{50} value of 14 nM, followed by ODN-furan with an IC_{50} value of 48 nM (Table 1). ODN-north shows the least inhibitory activity. It has no detectable inhibitory activity at concentrations below 75 nM and an estimated IC_{50} value of ~180 nM.

ODN binding to M.*Hha*I was assessed by incubating the enzyme with each ODN (-north, -south, and -furan) in the absence (binary complex) or presence of cofactor, AdoMet or AdoHcy (ternary complex), for 30 min. The complexes with bound ODN were separated from free ODNs by polyacrylamide gel electrophoresis under nondenaturing conditions (Figure 3). Since the same ^{32}P-radiolabeled complementary strand was used to form each of the ds-ODNs used in this study, the amount of complex formation with each type of ds-ODN can be compared directly by autoradiographic quantitation of the amount of radiolabel associated with the complex. The inference that M.*Hha*I bound to DNA is in an "open" or "closed" conformation is made on the basis of the complex's electrophoretic mobility in the gel.[9] Ternary complexes between M.*Hha*I, ds-ODN-C (cytosine target) and AdoHcy migrate faster than binary complexes formed without cofactor.[10,58] The more rapidly migrating complex is presumed to be more compact because it has a structure corresponding to the crystallographically determined structure of ternary complexes between M.*Hha*I, ds-ODN-C, and AdoHcy. In this complex, two regions of the enzyme, the flexible active site loop (amino acid residues 80−99) and the small domain recognition loop (amino acid residues 231−238), have undergone conformational changes relative to their positions in the X-ray crystal structure of M.*Hha*I with cofactor alone. The loops "close" around the DNA strand with the completely flipped target base (or abasic sugar moiety), occupying its position in the helix and "locking" it into the active site pocket. The more slowly migrating binary complex is presumed to be in a less compact "open" or nonlocked conformation.[9]

Interestingly, both ODN-south and ODN-furan bind to M.*Hha*I and form a "closed" complex regardless of whether cofactor is present or not (Figure 3, lanes 2−4 and 10−12),

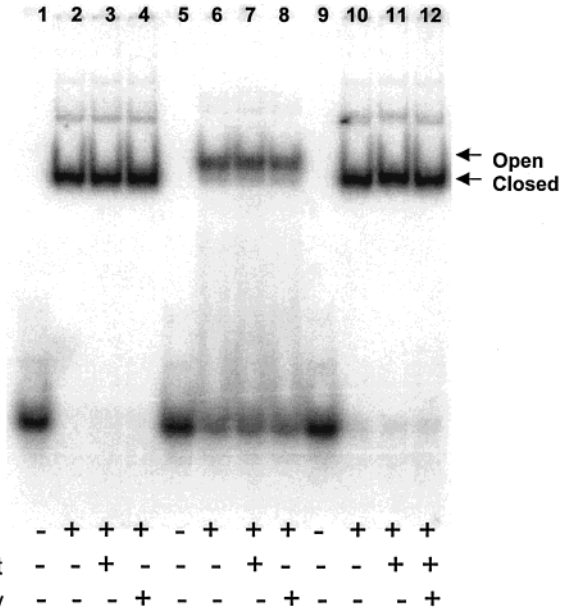

Figure 3. Comparison of the formation of binary (no cofactor) and ternary (with AdoMet or AdoHcy) complexes between M.*Hha*I and ODNs-furan (lanes 2−4), -north (lanes 6−8), and -south (lanes 10−12). All ODNs were radiolabeled on the methylated complement strand so that the amount of the different ODNs bound into complexes could be directly compared without need to adjust for variations in efficiency of radiolabeling. Lanes 1, 5, and 9 show the migration of the ds-ODNs in the absence of enzyme. Lanes 2, 6, and 10 are minus cofactor. Lanes 3, 7, and 11 are +AdoMet and lanes 4, 8, and 12 are +AdoHcy. Position of "open" and "closed" complexes is indicated by arrowheads. Details for complex formation and electrophoretic separation are given in Methods.

suggesting that the active site loop can assume a conformation similar to that observed in the crystal structure of the ternary complex.[1] Complexes containing ODN-north bound to M.*Hha*I display the unique characteristic of binding primarily as an "open" more slowly migrating conformation under all three conditions (lanes 6−8). Although a small proportion (~10%) of the more rapidly migrating complex is detectable, its formation is not enhanced in the presence of cofactor. This suggests that cofactor cannot facilitate the conformational change of the flexible, active site loop of the enzyme around the helical structure formed by ODN-north. However, the enzyme appears capable of adopting a closed conformation upon binding to a small population of north abasic targets that have achieved a fully flipped conformation despite the restraints imposed by the constrained north pseudosugar (see below).

ODN-north also differs from ODN-furan and ODN-south in its binding capacity. In either the presence or absence of cofactors, binding of M.*Hha*I to ODN-south or ODN-furan in a closed conformation was quantitative (~98% input = 100-(ODN bound/ODN bound + ODN free) with equimolar concentration of enzyme and ODN. Under the same conditions, 54% of ODN-north was bound in the "open" complex in the absence of cofactor, 55% in the presence of AdoMet, and 47% in the presence of AdoHcy. Binding to ODN-south and ODN-furan is essentially irreversible. In the absence of cofactor, it takes more than 110 h for 50% dissociation of ODN-south and 55 h for ODN-furan to dissociate from M.*Hha*I when incubated in the presence of 100-fold excess of cold competitor ODNs. In contrast, the dissociation of the 10% of closed binary complex formed by ODN-north has a $T_{1/2}$ of ~14 h. under the same conditions. The $T_{1/2}$ for the "open" complex of ODN-north is too small to be measurable (data not shown).

(58) Mi, S.; Alsono, D.; Roberts, R. J. *Nucleic Acids Res.* **1995**, *23*, 620−627.

Table 2. Averages of Bend Angles between Base Pair 2 and Base Pair 11 Normal Vectors and RMSD from B-DNA and A-DNA in the Final 1500 ps of DNA System Simulations[a]

	mean bend angle (deg)	RMSD[b] (Å) from B-DNA	RMSD[b] (Å) from A-DNA
1. control	18.1 (0.4)	3.3 (0.1)	4.8 (0.1)
2. furan	16.6 (0.8)	2.9 (0.1)	4.4 (0.1)
3. north	20.1 (0.8)	3.2 (0.1)	4.2 (0.1)
4. south	21.4 (1.4)	3.1 (0.1)	4.2 (0.0)

[a] Standard errors in parentheses. [b] RMSD, root-mean-square deviations.

It should be noted that the binding affinity of these ODNs for M.*Hha*I (south > furan ≫ north) is directly related to the inhibitory activity of the three abasic ODNs (south > furan ≫ north). However, it is not directly related to their melting temperatures, which are ranked north > south > furan (Table 1). Furthermore, the melting temperatures of all three abasic ODNs are reduced by ∼18 ± 1.4 °C relative to ODNs with the same structure containing a cytosine base as target. It is unlikely that a 1.4 °C difference in melting temperature between ODN-south and ODN-furan would decrease the $T_{1/2}$ for dissociation only 2-fold while the same difference in melting temperature between ODN-north and ODN-furan would decrease the $T_{1/2}$ from more than 50 h for dissociation of ODN-furan complexes to less than 1 min for dissociation of the bulk of ODN-north complexes. The results are consistent with formation of a highly stable "closed" complex with ODN-south and ODN-furan that leads to rapid enzyme inactivation. They also suggest that some intrinsic property of the north-constrained abasic sugar, other than its influence on the stability of the helix, is responsible for the observed preponderance of the relatively unstable "open" complex of enzyme with ODN-north.

Computational studies of the ODNs in aqueous solution were undertaken to determine how constraining the abasic sugar conformation influences the structural and dynamic properties of the DNA, thereby leading to the biochemical properties discussed in the preceding section. Calculations on the ternary complexes were also performed to investigate the impact of the constrained pseudosugars when the ODN is bound to M.*Hha*I. DNA−protein interactions are also expected to impact the biochemical results.

3. Computational Studies. 3.1. DNA in Aqueous Solution. Substitution of an abasic sugar into the backbone has been shown to cause minor overall structural deformation of the double-helical form of the DNA.[57] To identify possible large-scale structural deformations in the present systems, two parameters were assessed: (a) the bend angles between the penultimate base pairs of the ODNs and (b) the root-mean-square difference (RMSD) values with respect to canonical B-DNA and A-DNA for non-hydrogen ODN atoms (Table 2). There were no significant differences between these parameters for the ODN-abasic systems and the ODN-C system. This indicates that the absence of a base in the abasic systems does not cause significant overall distortion of the DNA duplex. Even the presence of a conformationally constrained A-DNA-like north carbocyclic sugar in the otherwise B-DNA-like duplex does not cause any significant bending in the DNA. The RMSD values also indicate that the DNA adopts a form intermediate to the canonical B-DNA and A-DNA forms, consistent with previous studies.[42]

Flipping out of the target sugar from the interior of the canonical DNA duplex structure is critical to the methylating activity of M.*Hha*I.[1] The extent of flipping was estimated by measuring the sugar O4′−O4′ interstrand distance during the MD simulations; in the north and south sugars the carbon-labeled C* in Figure 2 is used instead of the O4′ atom (see Methods). Figure 4 shows the probability distribution of the sugar O4′−O4′ distances observed for the four ODNs along with vertical lines indicating the O4′−O4′ distance in canonical B-DNA and the abasic DNA−M.*Hha*I complex. It is clear that the sugar which shows the maximum propensity for flipping out of the helix is that in ODN-furan followed by ODN-south. At certain time points, however, the ODN-south flips out to a similar extent as the completely flipped ODN-furan (i.e., an O4′−O4′ distance of ∼18 Å). ODN-north, on the other hand, shows a lesser tendency to flip out and dwells predominately inside the duplex structure. The ODN-north does, however, show short excursions to a partially flipped-out state (O4′−O4′ distance ∼15 Å) without ever flipping out completely. ODN-C, with a sharp peak centered around ∼12.8 Å, shows no tendency to flip out spontaneously on the observed time scale of the simulation, consistent with experimental studies showing a millisecond time scale of spontaneous base flipping.[59,60]

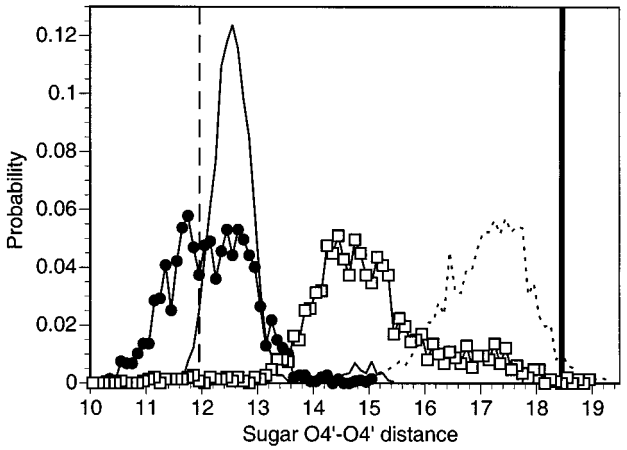

Figure 4. Probability distribution of sugar O4′−O4′ distances in the four DNA system MD simulations. The lines and symbols used for the different systems are as follows: control DNA system, line; furan DNA system, dashed line; north DNA system, (●); south DNA system, (□). Sugar O4′−O4′ distance in angstroms; bold vertical line, furan ternary crystal structure sugar O4′−O4′ distance; dashed vertical line, canonical B-DNA structure sugar O4′−O4′ distance.

To identify the local phosphodiester dihedrals that may impact flipping, phosphodiester dihedrals were obtained from the flipped region of the DNA for nine DNA-methyltransferase crystal structures.[1,2,10,61−64] The average values over those nine structures with the target site in the flipped-out form along with B-DNA modal values are presented in Figure 5 along with a diagram showing the corresponding dihedrals in DNA. Comparisons of flipped and B-form dihedrals show the differences to be localized to a few torsions. These are presented in boldface type in Figure 5. For the flipped sugar, there are significant differences in γ and ζ. Beyond the flipped sugar position, significant changes also occur in the adjacent 5′-ϵ and 3′-β dihedrals. On the basis of the similarity of these differences in

(59) Guéron, M.; Kochoyan, M.; Leroy, J.-L. *Nature* **1987**, *328*, 89−92.
(60) Moe, J. G.; Russu, I. M. *Biochemistry* **1992**, *31*, 8421−8428.
(61) O'Gara, M.; Klimasauskas, S.; Roberts, R. J.; Cheng, X. *J. Mol. Biol.* **1996**, *261*, 634−645.
(62) O'Gara, M.; Roberts, R. J.; Cheng, X. *J. Mol. Biol.* **1996**, *263*, 597−606.
(63) Kumar, S.; Horton, J. R.; Jones, G. D.; Walker, R. T.; Roberts, R. J.; Cheng, X. *Nucleic Acids Res.* **1997**, *25*, 2773−2783.
(64) Sheikhnejad, G.; Brank, A.; Christman, J. K.; Goddard, A.; Alvarez, E.; Ford Jr., H.; Marquez, V. E.; Marasco, C. J.; Sufrin, J. R.; O'Gara, M.; Cheng, X. *J. Mol. Biol.* **1999**, *285*, 2021−2034.

Residue	Dihedral	BDNA	Crystal
5'	alpha	298	289 (9)
	beta	168	182 (6)
	gamma	51	62 (5)
	delta	143	153 (3)
	epsilon*	**187**	**264 (3)**
	zeta	262	288 (3)
Flipped	alpha	298	276 (5)
	beta	168	193 (4)
	gamma*	**51**	**180 (4)**
	delta	143	77 (3)
	epsilon	187	202 (6)
	zeta*	**262**	**95 (7)**
3'	alpha	298	258 (7)
	beta*	**168**	**228 (6)**
	gamma	51	74 (5)
	delta	143	144 (2)
	epsilon	187	185 (3)
	zeta	262	263 (4)

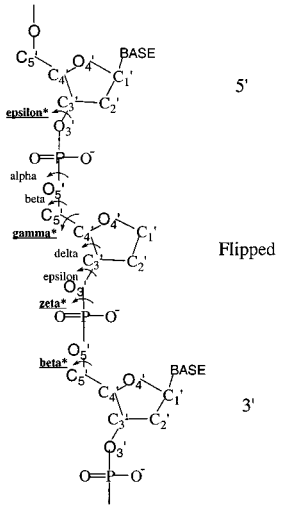

Figure 5. Averages of flipped region backbone dihedrals and modal B-DNA values. The diagram on the right indicates the position of these dihedrals along the backbone with the dihedral degrees of freedom denoted by curved arrows. Significantly distorted dihedrals indicated in boldface type with a following asterisk. Note: Distortion in the δ-dihedral of the flipped sugar is associated with the pseudorotation angle of the sugar. The pseudorotation angle properties are discussed later and therefore the δ-dihedral is not indicated in boldface type here. The individual dihedral values for the experimental structures, from which the averages shown here were obtained, are listed in Table 1 of the Supporting Information. Standard errors are in parentheses.

the nine structures, as evidenced by the small standard errors (see Table 1 of the Supporting Information for primary data), these specific dihedrals would be expected to have the largest impact on the flipping event.

The pathway of flipping in all three abasic DNA systems was through the minor groove, as confirmed by visual inspection of intermediate conformations during the flipping process (not shown). The three ODNs, however, show significant differences in the sequence of changes in the phosphodiester backbone dihedral angles asssociated with flipping of the sugar. Analysis of the O4′−O4′ distance time series for the flipped sugars along with the time series for the phosphodiester backbone dihedrals that show significant distortions in the crystal structures (Figure 2 of Supporting Information) indicates differences that are consistent with the survey results. For ODN-furan and ODN-south, changes are observed in γ; however, significant differences in the time series are also present in the other dihedrals, indicating that flipping occurs via different pathways. No corresponding dihedral transitions occur in ODN-C or ODN-north, consistent with the lack of significant flipping of the sugar in these systems. Thus, the dihedral angles showing alterations associated with sugar flipping in the simulations are consistent with those observed to be distorted in experimental crystal structures. Furthermore, on the basis of the pseudorotation angle time series (not shown), no significant change in sugar pucker from a south conformation is required for flipping.

Of the differences in phosphodiester backbone dihedrals observed both experimentally and in the calculations, it may be assumed that the structure of the sugar will impact the inherent conformational properties of the dihedrals closest to the sugar moiety. On the basis of this assumption, changes in the inherent conformational properties of the γ-dihedral of the flipped sugar were suspected to influence the different flipping properties of the sugar in the three abasic simulations.

Investigation of the influence of sugar structure on the conformational properties of the γ-dihedral was performed via

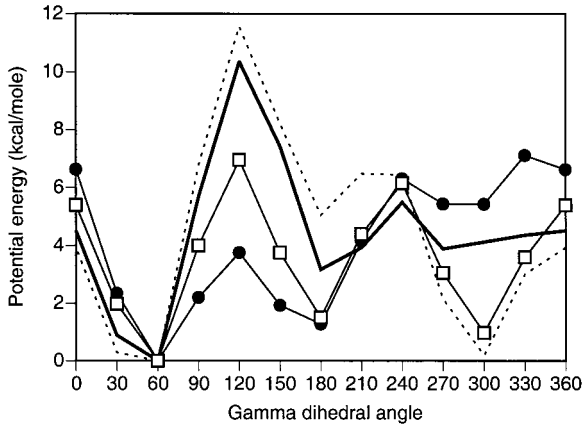

Figure 6. Potential energy as a function of the γ-dihedral in model compounds. Symbols are as follows: abasic furanose compound A with the constrained south sugar conformation, dashed line; abasic furanose compound A with the constrained north sugar conformation, bold line; north carbocyclic compound B (●); and south carbocyclic compound C (□). Dihedral angles in degrees.

ab initio quantum mechanical calculations on model compounds A, B, and C (Figure 2). Potential energy profiles for γ for the abasic furanose compound A, north carbocyclic compound B, and south carbocyclic compound C are shown in Figure 6. Due to the flexibility of the furanose sugar moiety and to allow for systematic analysis of the effect of sugar conformation on the behavior of the γ-dihedral, an additional ring constraint was applied to explicitly sample the C2′ endo and C3′ endo ring conformations in compound A. Comparison of the four surfaces shows the chemical structure of the sugar moiety to significantly influence the energetic properties. Common to all surfaces are the three minima that occur around 60, 180, and 300°, corresponding to the gauche$^+$, (g^+), trans (t), and gauche$^-$ (g^-) states, respectively. The g^+ minimum corresponds to the conformation observed in experimental DNA duplex structures.[13] Of note is the energy of the g^- minimum in compound B (north), which is ∼6 kcal/mol greater than that of both compound A (furan) with the south constraint and compound C (south). Interestingly, the high energy of the g^- minimum (∼4 kcal/mol greater than the g^+ minimum) is also observed in compound A when the sugar moiety is constrained to be north, indicating that the observed high energy of the g^- state is closely associated with the north sugar conformation. The elevated energy g^- minimum in compound B is suggested to disallow the transition to the g^- γ-conformation in ODN-north. In the MD simulations, ODN-furan and ODN-south, which show significant flipping, exhibit sampling of the g^- state of the γ-dihedral (γ-dihedral value ∼300° in Figure 2 of the Supporting Information). ODN-C and ODN-north, which do not show significant flipping of the sugar, do not show sampling of the g^- state. On the basis of these observations, the transition to the g^- state of the γ-dihedral may contribute to the flipping process. The inability of the north carbocyclic sugar to attain the g^- state due to its intrinsic energetics is suggested to hinder flipping of the north carbocyclic sugar out of the DNA duplex. The role of the north conformation of the sugar on the g^- state is supported by the high energy of that state when the sugar in compound A is constrained to the north conformation. This is consistent with results from the MD simulation where the ODN-furan sugar conformation remains south during the flipping process (not shown), thereby avoiding the high energy g^- state associated with the north conformation.

Probability distributions of the four dihedrals that differ from canonical values in the crystal structures (see Figure 5) for the

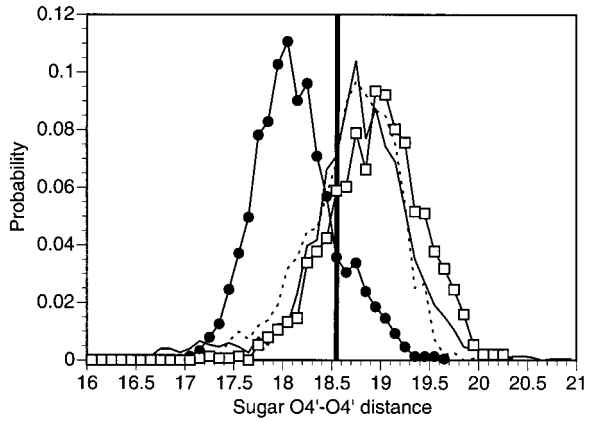

Figure 7. Probability distribution of sugar O4′−O4′ distances in the four ternary system MD simulations. The symbols for the different systems are as follows: control ternary system, line; furan ternary system, dashed line; north ternary system (●); south ternary system (□). Sugar O4′−O4′ distance in angstroms; bold line, furan ternary crystal structure sugar O4′−O4′ distance.[11]

last 1500 ps of the ODN simulations along with values observed in B-form and flipped-out DNA experimental structures were analyzed (see Figure 3 of the Supporting Information). For the 5′-ϵ and 3′-β dihedrals, only ODN-furan and ODN-south show significant sampling of states around the DNA−M.*Hha*I complex average values. This is consistent with the observation that only these two ODNs show complete flipping of the abasic sugar. For the γ-dihedral, only ODN-furan and ODN-south populate the *t* state, though the amount of sampling is small. ODN-south alone shows some sampling of the g^+ state of the ζ-dihedral at a value lower than the experimental average. These probability distributions indicate that only ODN-furan and ODN-south spontaneously sample the backbone conformations seen in the DNA−M.*Hha*I complexes with ODN-south showing a greater tendency to sample those conformations.

3.2. DNA in Ternary Complex. Understanding of the structural and dynamic behavior of the DNA in the ternary complexes, in addition to its behavior alone in aqueous solution, is necessary to interpret the biochemical observations. All ternary complex MD simulations were started from the flipped out form of the sugar seen in the crystal structures. The sugar O4′−O4′ distance, used to monitor the flipping-out transition in the DNA MD simulations, was assessed to detect any characteristic behavior for the ternary complexes. Figure 7 shows the probability distributions of the sugar O4′−O4′ distances for the four ternary complex simulations along with the experimental structure value. The ternary-north system shows a small shift toward a lower value for the sugar O4′−O4′ distance as compared to the other three systems. The presence of the deviation indicates that the flipped region in the north ODN is attempting to revert back to the non-flipped-out conformation.

Probability distributions of the four dihedrals that differ from canonical values in the crystal structures (see Figure 5) were determined for the ternary simulations (Figure 4 of the Supporting Information). Of the four dihedrals, significant deviations from the experimental flipped-out structure average values are observed in the flipped position γ- and ζ-dihedrals. In both ternary-C and ternary-furan, the flipped position γ-dihedral shows a tendency to populate a region close to the g^+ state seen in experimental B-DNA structures. In ternary-north, the γ-dihedral populates the *t* state but at a lower value (∼150 °) than the experimental *t*-state γ-value. The ternary-south γ-dihedral populates both the *t* and g^- states with the *t*-state population showing excellent correspondence with the experimental average. For the flipped position ζ-dihedral, ternary-C and ternary-south show a preference for the g^+ state but with a lower value than experimental average values. It is to be noted that ternary-south does show some sampling of a state intermediate to the g^+ and *t* states of the ζ-dihedral. In ternary-furan, the ζ-dihedral populates both the g^- and g^+ states. In ternary-north, the ζ-dihedral occupies the *t* state exclusively. For all four dihedrals selected, ternary-south shows the best agreement with the experimental flipped-out average values.

Table 3. Average Interaction Distances (Å) between Gln237 and Ser87 or Guanine 7 from the Ternary Simulations[b]

interaction	control	furan	north	south
Gln237 Nϵ2 to Ser87 Oγ	4.05 (0.15)	4.81 (0.07)	5.20 (0.13)	3.25 (0.02)
Gln237 N to Gua7 O6	2.89 (0.01)	2.83 (0.00)	3.03 (0.02)	2.85 (0.01)
Gln237 Oϵ1 to Gua7 N1	2.85 (0.01)	2.88 (0.01)	2.87 (0.00)	2.83 (0.00)
Gln237 Oϵ1 to Gua7 N2	3.09 (0.02)	3.31 (0.03)	3.05 (0.03)	3.31 (0.02)

[b] Standard errors in parentheses.

Previous studies have implicated a role of Gln237 in stabilizing the ternary complex.[58] This stabilization by Gln237 is facilitated by interactions with the "orphan" guanine base and with the flexible active site loop via residue Ser87. Analysis of these interactions from the ternary MD simulations is presented in Table 3 as average interaction distances. Consistent with the biochemical binding data, the shortest interaction distance involving Ser87 occurs with ternary-south and the longest with ternary-north, with the ternary-furan intermediate. Of note is the ternary-C distance being shorter that the ternary-furan distance, suggesting that the increased flexibility of this abasic furan may destabilize this particular interaction. Concerning interactions between the guanine base and Gln237, the interaction distances are similar in all four systems, indicating the lack of the target base and the different sugar structures to not significantly impact these interactions.

3.3. Pseudorotation Angle. The flipped-out abasic sugar adopts a north conformation in the crystal structure,[11] in contrast to the south conformation characteristic of B-DNA. Therefore, this pseudorotation behavior may be related to the conformational preference of the flipped-out sugar after conclusion of the flipping event. Probability distributions of the pseudorotation angle of the flipped position for all MD simulations were determined (Figure 5 of the Supporting Information). For the DNA simulations, it is clear that the south conformation is generally preferred in ODN-C, ODN-furan, and ODN-south. In ODN-north, the pseudorotation angle of the abasic sugar moiety exclusively populates the north conformation, consistent with the constrained nature of the carbocyclic sugar. In ODN-south, the sugar pseudorotation angle shows minor sampling of the north form due to a boat−chair transformation of the bicyclo[3.1.0]hexane ring system. The north form of the south carbocyclic sugar is very short-lived as expected from ab initio studies and experimental observations.[15−31,47] The wide distribution of the pseudorotation angle in ODN-furan is indicative of the abasic furanose ring being more flexible than the abasic north and south carbocyclic pseudosugar rings. Overall, the sugar moiety primarily samples the south form, consistent with B-form structures, except with the north DNA system where the chemical structure of the carbocyclic moiety enforces the north conformation.

In the ternary complexes, ternary-C samples pseudorotation angles intermediate to the north and south forms. A tendency

to sample the north conformation is indicated with brief excursions to the north form that occurs in the crystal structure.[1] In ternary-furan, the sugar makes a transition from the north form to the south form after ~300 ps (not shown) and remains in the south form for the remainder of the simulation. This is contrary to what is observed in the crystal structure and is probably a reflection of the more flexible nature of the abasic furanose sugar moiety. This presence of the south conformation, however, does not affect the sugar O4′−O4′ distance (Figure 7). For ternary-north, the expected north conformation is sampled throughout the simulation. Finally, the south ternary system shows the south conformation to dominate, consistent with the constrained carbocyclic structure. It is observed, however, that significant sampling of the north conformation occurs. These results indicate that, in the ternary complex, the north conformer of the sugar may be favored. However, the sampling of the south conformation in the furan ternary complex is not consistent with the observed crystal structure with the M.*Hha*I−abasic DNA−AdoHcy ternary complex (see below).

Discussion

Influence of Abasic Site on Duplex Stability. T_m measurements (Table 1) indicate that the presence of any abasic site is sufficient to strongly destabilize the duplex DNA, probably due to the loss of base stacking and Watson−Crick hydrogen bonding. Among the abasic ODNs, the order of stability was north > south > furan. These results are inversely correlated with the propensity for flipping calculated for the three systems (Figure 4), where the order is furan > south > north, but not the inhibitory capacity, where the order is south > furan > north. Although it is clear that the difference in T_m is not sufficient to account for the difference in binary and ternary complex stability observed in our biochemical studies, this result does suggest that spontaneous flipping can have a small but measurable impact on the overall stability of the DNA duplex.

Inhibition of M.*Hha*I by DNA Containing Abasic and Carbocyclic Pseudosugar Analogues at the Target Site. From the synthetic and biochemical experiments, the order of inhibitory potency was found to be ODN-south > ODN-furan ≫ ODN-north (Table 1 and Figure 1 of the Supporting Information). This result was surprising due to crystallographic data indicating that M.*Hha*I bound to DNA with either a flipped cytosine or an abasic site at the target position has the sugar in the north conformation.[11] To understand the rank order of binding, MD simulations were performed on the ODNs alone in solution and in a ternary complex with M.*Hha*I. The MD simulations reported here suggest that the sugar moiety in ODN-south and ODN-furan flips out of the DNA duplex spontaneously (Figure 4), a process that does not occur in ODN-north. To understand the cause of this difference, dihedrals in the phosphodiester backbone that change significantly upon binding of DNA to M.*Hha*I based on crystal structures were identified (Figure 5) and shown to undergo transitions in the MD simulations in which flipping occurs (Figure 2 of the Supporting Information). Of these dihedrals, γ is directly adjacent to the sugar moiety and, therefore, most likely to be influenced by the sugar structure. QM calculations on model compounds (Figure 2, compounds A−C) showed that the presence of the north carbocyclic sugar disfavors the g^- conformer of the γ-dihedral (Figure 6), thereby hindering flipping of the north carbocyclic sugar out of the DNA duplex. Constraining the abasic sugar to the north conformation yielded a similar result (Figure 6), indicating the hindered rotation to be due to sugar conformation rather than the chemical structure of the north carbocyclic sugar. Thus, enhanced binding of ODN-south and ODN-furan is due to the ability of the sugar to spontaneously flip out of the DNA duplex. Such flipping cannot occur with ODN-north due to hindered rotation about the γ-dihedral due to the ring conformation, leading to its significantly decreased binding.

Analysis of the conformations of the phosphodiester backbone of the target region in both DNA in solution (Figure 3 of the Supporting Information) and in the DNA−M.*Hha*I−AdoHcy complex (Figure 4 of the Supporting Information) from the MD simulations yielded information on the enhanced binding of ODN-south over ODN-furan. From the probability distributions of these dihedrals it was observed that ODN-south assumed conformations more similar to those that occur in DNA−M.*Hha*I−AdoHcy crystal structures than ODN-furan. Improved sampling of the bound conformation of the DNA phosphodiester backbone by ODN-south, therefore, is suggested to lead to the improved binding over ODN-furan. Thus, the overall binding profile from the biochemical studies is predicted to result from the capacity of the target site in the ODN to assume the protein-bound (flipped) conformation in solution and maintain that conformation when bound to the enzyme.

Propensity for the "Open" versus "Closed" Conformations of M.*Hha*I. An essential step in the mechanism of methyl transfer by M.*Hha*I is converting from an "open" complex with DNA to a catalytically competent "closed" complex when cofactor is available.[9] The gel-shift assay experiments reported here (Figure 3) show that M.*Hha*I assumes a closed conformation when bound to ODN-south and ODN-furan either in the presence or absence of cofactor. In contrast, M.*Hha*I bound to ODN-north is found predominantly in the open state in all cases. The formation of closed binary complexes between ODN-south and ODN-furan and M.*Hha*I is especially interesting since the normal substrate, ODN-C, requires the presence of AdoHcy to form a complex with closed conformation. From MD simulations it was observed that both ODN-south and ODN-furan assume a flipped out conformation in solution (Figure 4) and maintain the conformation in the ternary complex (Figure 6). This suggests that formation of the closed complex requires a totally flipped-out state. In ODN-north, since the carbocyclic sugar does not flip out of the duplex during the time of observation (Figure 4), this observation would predict that a closed conformation cannot form readily. In the ternary complex, the north sugar moiety shifts to shorter O4′−O4′ distances (Figure 6), suggesting that it does not want to assume that flipped-out conformation, which is consistent with the native gel-shift assay results on the ternary complexes.

Despite the predictions of the model, a small amount of closed conformation of ODN-north is observed in the gel assay. While the possibility that the north sugar moiety can assume a completely flipped-out state, compatible with the closed conformation, cannot be excluded due to limitations in the present calculations, this divergence between theory and experiment suggests that additional interactions may be contributing. One possibility is that interactions between Gln237 and the unpaired G residue at the abasic site not only favors the partial flipping that leads to formation of the "open" complex but allows the north constrained abasic to sample the completely flipped state. This is supported by the presence of this interaction in the ternary-north simulation (Table 3). Alternatively, in the absence of base, the enzyme may possibly take an active role in "flipping". What is clear is that, once achieved, the ODN-north in the "closed" complex becomes resistant to rapid exchange as evidenced by the $T_{1/2}$ for dissociation of ~14 h.

Preferred Sugar Pseudorotation Angles. As shown in Figures 2−4 of the Supporting Information, the present MD simulations reproduce a number of structural properties observed in DNA−M.*Hha*I crystal structures. Inconsistencies between the crystal structures and ternary MD simulations are, however, observed in the flipped furanose sugar pseudorotation angles (Figure 5 of the Supporting Information). On the basis of the ab initio calculations, the flipping process appears to be favored by the south sugar pucker (vide infra); however, the crystal structure[11] of the abasic ternary complex indicates the flipped sugar to assume a north conformation. In the ternary-furan MD simulation, however, the sugar primarily samples the south conformation. This tendency may be attributed to any of the following reasons: (a) overstabilization of the C2′ endo form of the sugar in the CHARMM force field parameters; (b) the limited time scale of the simulation that is not sufficient to represent the proper balance between the south and north conformations; (c) inherent flexibility in the conformation of the abasic sugar in the ternary complex not captured in the crystal structure;[11] and (d) the limited resolution of the crystal structure (2.39 Å), [11] which may make unambiguous assignment of the sugar pucker difficult. In this regard, it is of interest to note that recently published APE1−DNA complex structures show abasic flipped-out furanose sugars in the south conformation.[65] Although the test ODN had a different sequence from the one used in our studies, this finding suggests that for the flexible furan moiety either the north or south conformation is compatible with the flipped-out orientation of the sugar and that, during crystallization, either form could be trapped. Interestingly, brief excursions to the north conformation in the south carbocyclic sugar occur in the ternary-south simulation, which are not expected given the significantly greater stability of the rigid south conformation (Figure 5 of the Supporting Information). Moreover, the control ternary flipped sugar populates pseudorotation angles intermediate between the south and north forms, while the north carbocyclic sugar pseudorotation angle remains in the expected north conformation. These observations, along with the north conformation observed in X-ray crystal structure, suggest that, in the ternary complex, the north form of the flipped sugar is favored over the south form, though the present results support the possibility that the south conformation is compatible with the completely flipped-out state of the abasic sugar.

Model for the Structural Mechanism of M.*Hha*I. A proposed structural pathway for formation of a catalytically competent complex between M.*Hha*I, substrate DNA, and cofactor involves formation of at least two structurally distinct complexes prior to the attainment of the structural relationship between substrate, enzyme, and cofactor that is required for methyl transfer.[9] They are a recognition complex in which the target base remains stacked in an intact B-helix and an "open" conformation with substrate conformers with varying degrees of target base flipping. By combining information obtained in our biochemical and theoretical studies, we can expand on the following aspects of this model.

Enzymatic Influence on Direction of Flipping. On the basis of considerations of steric crowding, flipping of a target base through the major groove has been predicted to be more energetically favorable than flipping out through the minor groove.[66] Some enzymes, such as uracil glycosylase use a major groove-based mechanism to flip out their target bases[6] and may actively participate in base flipping.[67] However, the structural models for M.*Hha*I and M.*Hae*III make it likely that DNA cytosine (C5)-methyltransferases flip target cytosines through the minor groove.[1] Although NMR studies suggest that M.*Hha*I does not accelerate flipping of the target cytosine,[9] they cannot rule out the possibility that the enzyme is necessary to direct flipping of the target base toward the minor groove side.

The MD simulations in this study indicate that, at least in the absence of a base, sugar flipping occurs through the minor groove of DNA without requiring interaction with the enzyme. On the basis of visual inspection, when flipping occurs via the minor groove, the partially flipped-out form of the sugar appears to occupy the spatial region that the flexible active site loop (residues 80−99) closes around. Our calculations are not sufficient to give information about protein−DNA interactions in the recognition or the "open" complex. However, if we make the assumption that during the flipping process the flexible active site loop occupies the conformation seen in the binary M.*Hha*I−AdoMet complex, we can predict that this loop can only lock the enzyme in the "closed" conformation when the sugar (and base) is completely flipped out of the helix. This observation is consistent with the present biochemical studies that indicate that the enzyme in the ternary-north complex is found primarily in an "open" conformation, which is due to incomplete flipping of the north constrained analogue.

Recognition and Formation of "Open" Complexes. The initial binding of the M.*Hha*I recognition sequence GCGC in DNA is thought to be mediated primarily via major groove interactions with the small domain (residues 194−275) of the enzyme.[1] This region contains most of the sequence-specific contacts and, on the basis of ternary complex crystal structures, is proposed to remain in contact with the nontarget strand throughout the process of methyl transfer. This is consistent with the observation that, in the ternary complexes, where all sugars and the control cytosine are in the completely flipped configuration, the interaction distances between Gln237 and the orphan guanine base are similar for all four systems (Table 3).

All of our simulations of target flipping in solution indicate that the north constrained abasic target remains primarily inside the duplex DNA with short excursions to a partially flipped-out state (Figure 4, O4′−O4′ distances out to 15 Å). It is never observed in the completely flipped-out state during the time of observation. This is consistent with the gel-shift experiments where at least 50% of the ODN is found migrating as an "open" conformation while less than 10% is in the "closed" conformation in either the binary or ternary complexes. Previous studies with a base-paired C target have shown that the small amount of binary complex formed is in the open conformation while, upon formation of the ternary complex, the closed conformation dominates.[9] These results suggest that the open conformation is due to the sugar (and base in the normal substrate) occupying unflipped or partially flipped states that disallow closure of the flexible, active site loop around the target sugar and base. In the normal C substrate, the presence of cofactor stabilizes the interaction of the base with the protein, yielding a totally flipped conformation of the base and sugar, thereby allowing full closing of the flexible loop.

Formation of "Closed" Complexes. If, as postulated above on the basis of simulation data, complete flipping of the target sugar is necessary for formation of the "closed" conformation between ODN and M.*Hha*I, it would be predicted that the furan and south constrained abasic sites would preferentially form

(65) Mol, C. D.; Izumi, T.; Mitra, S.; Tainer, J. *Nature* **2000**, *403*, 451−456.

(66) Ramstein, J.; Lavery, R. *Proc. Natl. Acad. Sci. U.S.A.* **1988**, *85*, 7231−7235.

(67) Stivers, J. T.; Pankiewicz, K. W.; Watanabe, K. A. *Biochemistry* **1999**, *38*, 952−963.

closed conformations. This is exactly what was observed in our native gel-shift analysis of complex formation. The fact that there is no evidence for an effect of cofactor on the equilibrium level of "closed" conformation indicates that cofactor is not necessary for either establishing or stabilizing the "closed" conformation of the enzyme when it is bound to the furan or south sugar analogues. In essence, the furan and abasic south targets may invite closure of the flexible and recognition loops around themselves by adopting a completely flipped-out orientation. The enhanced stability of "closed" complexes of M.*Hha*I with ODN-south relative to ODN-furan is suggested to be due to its ability to better sample the bound DNA conformation and the stronger interaction between Ser87 in the flexible loop and Gln287 in the recognition loop (Table 3).

A similar lack of need for cofactor in formation of the highly stable "closed" conformation was noted with ODNs containing the transition-state analogue 5,6-dihydo-5-azacytosine (DZCyt) as target base.[64] This suggests that formation of the closed state is based on the ability of the base to be stabilized in the active site pocket. DZCyt being a transition-state mimic allows this stabilization to occur in the absence of cofactor. In contrast, the normal C substrate requires cofactor to stabilize the interaction of the completely flipped-out base with the large domain of M.*Hha*I.

In the case of mismatched base pairs,[10] the proposed model also explains why the open conformation is observed in the absence of cofactor while the closed conformation is observed in its presence. There is a high probability that a mismatched base pair populates a variety of flipped states in the binary complex after initial binding of the protein. The partially flipped-out states of the target base prevent the closing of the flexible loop around the DNA, leading to the observation of the open state of the protein. The presence of the cofactor leads to greater stabilization of the completely flipped-out target base in the active site pocket, allowing the flexible loop to close around the DNA and form the closed complex. However, as described previously,[64] this complex is less stable than that formed with cytosine, presumably due to less than ideal interactions with the active site pocket.

Conclusion

The presence of conformationally constrained sugar substituents in DNA not only enforces the designated pseudorotation conformation in the sugar moiety but also results in changes in conformational flexibility of the γ-dihedral adjacent to the sugar substituent. Such alterations in intrinsic energetic properties associated with localized changes in DNA structure result in substantially different structural and dynamic behavior of the DNA. These structural and dynamic changes result in biochemical consequences including altered duplex DNA stability and changes in interactions of the DNA with M.*Hha*I. The combined synthetic, biochemical, and computational approach yields a unique view of how structural and dynamic properties of biomolecules impact biochemical properties. The present results are consistent with and extend a current model describing the structural mechanism(s) used by M.*Hha*I to ensure specificity and optimal alignment of target base and methyl donor during the methylation reaction.

Abbreviations: M.*Hha*I, *Hha*I DNA (cytosine-5)-methyltransferase; ODN, oligodeoxyribonucleotide; ss, single-stranded; ds, double-stranded; QM, quantum mechanics; MD, molecular dynamics; AdoHcy, *S*-adenosylhomocysteine; AdoMet, *S*-adenosylmethionine; 5mC or M, 5-methylcytosine; TBE, 89 mM Tris borate (pH 8.0), 2 mM EDTA; SSC, 45 mM sodium chloride, 4.5 mM sodium citrate; OD, optical density.

Acknowledgment. This work has been supported by NIH Grant GM-51501 and computational support from the Pittsburgh Supercomputing Center and the National Partnership for Advanced Computational Infrastructure to A.D.M.,Jr.; grant support from DAMD Breast Cancer Program-17-98-1-8215, the Susan G. Komen Breast Cancer Fund and the Nebraska Department of Health to J.K.C.; fellowship support from the Graduate College of UNMC to A.S.B.

Supporting Information Available: Text and two schemes describing results of the synthetic procedures, five figures and a table listing the values of the phosphodiester backbone in the vicinity of the flipped based for currently available crystal structures of the DNA−M.*Hha*I complexes, and the empirical force field parameters for the carbocyclic sugar analogues (PDF). This material is available free of charge via the Internet at http://pubs.acs.org.

JA001989S